Supporting Information

Aggregation of Microtubule Binding Repeats of Tau Protein is Promoted by Cu^{2+}

Soha Ahmadi[1,2], Shaolong Zhu[3,4], Renu Sharma[2], Bing Wu[1†], Ronald Soong[1,2] R. Dutta Majumdar[1††], Derek J. Wilson[3,4*], Andre J. Simpson[1,2*], Heinz-Bernhard Kraatz[1,2*]

[1] Department of Physical and Environmental Science, University of Toronto Scarborough, 1265 Military Trail, Toronto, Ontario, Canada
[2] Department of Chemistry, University of Toronto, 80 St. George St., Toronto, Canada
[3] Chemistry Department, York University, 4700 Keele Street, Toronto, ON, Canada
[4] The Centre for Research in Mass Spectrometry, York University, Toronto, ON, Canada
†Dutch-Belgian Beamline (DUBBLE), ESRF - The European Synchrotron Radiation Facility, CS 40220, 38043 Grenoble Cedex 9, France
††Bruker Ltd., 2800 High Point Drive, Suite 2016, Milton, ON, Canada

Table of Contents

- **Materials and methods**

All chemicals and reagents were analytical grade and obtained from Sigma Aldrich. Lipoic acid N-hydroxy succinimide ester (Lip–NHS) was synthesized as reported before.[1] Tau Peptide (244-274) (Repeat 1 domain, R1), Tau Peptide (275 - 305) (Repeat 2 domain,R2), Tau Peptide (306 - 336) (Repeat 3 domain,R3) and Tau Peptide (337 - 368) (Repeat 4 domain, R4) were purchased from Anaspec (Fremont, CA, USA). The masses and the purity of the peptides were confirmed by ESI-MS and HPLC (≥95%), respectively. See Scheme 1 for the amino acid sequence of R1-R4. All the chemicals used for gel electrophoresis were purchased from Bio-Rad Laboratories (Canada) Ltd. Millipore-Q water (18.2 MΩ cm) was used for sample preparation and all the experiments were performed at room temperature and pH 7.4 unless otherwise mentioned. A 10 mM $CuCl_2$ solution was prepared in Millipore-Q water right before each experiment and diluted in phosphate buffer, pH 7.4 to desire concentration. The peptide stock solutions were prepared by dissolving 1 mg of each peptide in Millipore-Q water to get a final concentration of 3 mM. The stock solutions were aliquoted and kept at -20 °C. The $CuCl_2$ solution was added to the peptide with the molar ratio 2:1 of Cu^{2+}:R to shift the equilibrium to the formation of the copper complex unless otherwise mentioned. All the samples were kept at room temperature for 24 hours before the experiment unless otherwise mentioned.

- **Mass Spectrometry**

Electrospray ionization mass spectrometry (ESI-MS) and ion-mobility spectrometry mass spectrometry (IMS-MS) were performed on Waters Synapt G1 with the following parameters: Capillary 2.5 kV, Sampling Cone 50.0V, Extraction Cone 1.0 V, Trap Collision Energy 15.0 V, Transfer Collision Energy 6.0 V, IMS Gas Flow 25.00 mL/min, IMS Wave Velocity 350 m/s, IMS Wave Height 10.0 V. [2-4]

Microtubule binding repeats R1-R4 (70 µM) were incubated with $CuCl_2$ solution (molar ratio 2:1 of Cu^{2+}:R) in order to shift the equilibrium to the formation of R-Cu complex for 24 hours at room temperature. For the control sample, microtubule repeat domains (R1-R4) were kept at the same condition in the absence of copper ions. All the solutions were diluted to the final concentration of 20 µM of peptide prior the analysis.

- **NMR Spectroscopy**

All experiments were performed on a Bruker Avance III 500 MHz (^{1}H Larmor frequency) NMR spectrometer, using ^{1}H-^{13}C-^{15}N TXI 1.7-mm microprobe fitted with an actively shielded Z-gradient, at a controlled temperature of 298 K (25 °C). The experiments were carried on 2 mM Microtubule repeat domains R1-R4 in phosphate buffer (pH 7.4) with or without Cu^{2+} ions. All samples were incubated for 16 hours prior to running the NMR experiments. Typical NMR experiments were run for 8 hours.

1D ^{1}H NMR

All 1D ^{1}H NMR spectra were acquired using the PURGE radio frequency (r.f.) sequence.[5] Typical parameters used to acquire the 1D 1H NMR spectrum are as followed: 1) A 57 kHz ^{1}H r.f. field strength 2) 20 ppm spectral width, 400 transients, 3) 32K acquisition points 4) 8.6 s delay between transients (which represents > 5 *T_1) 5) the transmitter offset was set to 4.706 ppm, which matches that of water. All NMR spectra were processed using an exponential function with a line broadening of 0.3 Hz and zero fill to 64K data points.

2D 1H T_1 Relaxation NMR experiments

The T_1 NMR experiments were performed using a standard inversion recovery experiment. Shaped presaturation and W5-watergate modified with a perfect echo[6] were added to the sequence to suppressed the water before acquisition. Typical parameters used for inversion recovery were: 1) A 57 kHz ^{1}H r.f. field strength 2) 20 ppm spectral width, 3) 16 transients 4) 32K acquisition points 5) 11s delay between transients 6) the transmitter offset was set to 4.706 ppm, which matched that of water. Presaturation of water was done via back to back 2.5ms square pulses applied back to back during the recycle delay. A total of 16 FIDs were collected for each of the relaxation experiments, and relaxation time (T_1) calculations were done on Bruker Dynamics Centre (v 2.4.5) using mono-exponential fitting functions [1]. The resultant files were exported into MS Excel for further analysis.

Fitting function for T_1: $I(t) = I(0) * [1 - 2 * \exp(-t/T_1)]$ [1]

2D 1H T_2 Relaxation NMR experiments

The T_2 NMR experiments were performed using a standard CPMG NMR experiments. Shape Pre-Saturation and W5-watergate modified with a perfect echo were added to the sequence to suppressed the water before acquisition. Typical parameters used for CPMG NMR experiments were: 1) A 57 kHz ^{1}H r.f. field strength 2) 14 ppm spectral width, 3) 64 transients, 4) 32K acquisition points 5) 11s delay between transients 6) the transmitter offset was set to 4.706 ppm 7) 1.2 ms echo delay period. The water pre-sat was done via back to back 2.5ms square pulse applied back to back during the recycle delay. A total of 16 FIDs were collected for the relaxation experiments and relaxation time (T_2) calculations were done on Bruker Dynamics Centre (v 2.4.5) using mono-exponential fitting functions [2]. The resultant files were exported into MS Excel for further analysis.

Fitting function for T_2: $I(t) = I(0) * \exp(-t/T_2)$ [2]

Diffusion Ordered Spectroscopy (DOSY)

DOSY was collected using a Bipolar Pulse Pairs Longitudinal Eddy Current Delay (BPPLED) sequence[7] with W5-watergate modified with a perfect echo[6] were added to the sequence for water suppression. Typical parameters used for DOSY experiments were: 1) A 57 kHz ^{1}H r.f. field strength 2) 14 ppm spectral width, 8 dummy scans, 128 transients, 3) 14K acquisition points 4) 3.1 s delay between transients 5) the transmitter offset was set to 4.706 ppm 6) 200 ms diffusion time 7) 2.5ms sine shaped gradient for diffusion encoding/decoding. The water pre-sat was done via back to back 2.5 ms square pulse applied back to back during the recycle delay. The indirect dimension was acquired under phase insensitive mode and a total of 24 increments were collected. All the DOSY data were processed using Bruker Dynamics Center (v 2.4.5) using a multi-exponential fitting.

Fitting Equation for D: $I(t) = I(0) * \exp(-DB)$, where $B = \gamma^2G^2\delta^2(\tau - \delta/3)$ [3]

- **UV-visible studies**

UV-visible experiments were done with Agilent Cary 60 UV-vis spectrophotometer using 1 cm quartz cuvette. The time dependent studies were performed using 100 µM concentration of ascorbic acid in the MES (2-(N-morpholino) ethanesulfonic acid buffer, pH 6. The concentrations of $CuCl_2$ solution and microtubule binding repeat R1-R4 solutions were 10 µM and 5 µM respectively. Ascorbic acid (100 µM) was added to the peptide solution after getting a stable absorbance. The absorbance signal of ascorbic acid at 265 nm was taken to monitor the redox activity of Cu^{2+} in R-Cu complexes. Control experiments carried out using a solution of 100 µM ascorbic acid and 10 µM $CuCl_2$

- **Fluorescence experiments**

Fluorescence studies were done with PTi Quantmaster 40 spectrofluorometer using 1 cm quartz cuvette.

ROS measurements

2',7'-dichlorodihydrofluorescein diacetate (H_2DCFDA) will be oxidized to the fluorescent 2',7'-dichlorofluorescein (DCF) in the presence of reactive oxygen species (ROS). In order to convert H_2DCFDA to DCF, the de esterification has been done by employing an alkaline hydrolysis protocol described in literature,[10,11] briefly 500 µL of 1 mM H_2DCFDA solution was added to 2 mL of 0.01 M NaOH. After 30 minutes, 10 mL of a 25 mM phosphate buffer at pH 7.4 was added to the H_2DCFDA/methanol/NaOH solution. Then 50 µL of this solution was added to the reaction solutions containing 5µM $CuCl_2$ and 5µM microtubule binding repeats R1-R4. The probe was excited at an excitation wavelength of 490 nm and emission spectrum was recorded in the wavelength range of 500-600 nm. The DCF fluorescence at 523 nm was utilized to monitor the ROS formation upon interaction of $CuCl_2$ with microtubule binding repeat R1-R4. Control experiments carried out using a solution of a) H_2DCFDA probe alone; b) H_2DCFDA acid with 5 µM $CuCl_2$; H_2DCFDA acid with 5 µM glutathione and c) H_2DCFDA with 5 µM of R1-R4; H_2DCFDA acid with 5 µM CuCl in 50 µM ascorbic acid/ 25 µM NaCl.

ThT fluorescence experiments

A stock solution of thioflavin T (ThT) was prepared in 50 mM phosphate buffer, pH 7.4 right before the experiment. The ThT solution was added to the peptide solution to the final concentration of 20 µM ThT, 45 µM peptide, and 25 mM phosphate buffer. The microtubule binding repeats R1-R4 solutions were incubated with or without Cu^{2+} (2:1 molar ratio of Cu:R) at room temperature for up to four days. Fresh R1-R4 solutions were used as control samples. The ThT fluorescence was monitor using excitation wavelength of 444 nm and the emission spectrum was recorded from 450 nm to 480 nm. The ThT fluorescence intensity at 483 nm was used to monitor the peptide aggregation.

- **Circular dichroism (CD) spectroscopy**

CD measurements were carried out using a Jasco J-815 CD spectrometer (JASCO, Tokyo, Japan) at 25 °C under a constant flow of nitrogen gas. The CD spectra were recorded between 185 and 700 nm using a 0.2 mm quartz cuvette. Microtubule binding repeat R1-R4 solutions (pH 7.4) were prepared at 0.14 mM concentration with or without $CuCl_2$ solution (molar ratio 2:1 of Cu^{2+}: R). The CD spectrum were recorded for each peptide every 15 min for 1 hour and after 24 hours incubation at room temperature. Each spectrum represents the average of 3 scans.

- **Electrochemical experiments**

Electrochemical studies were performed on a CHI 660C potentiostat (CH Instruments, Austin, TX) using a three-electrode set up enclosed in Faraday cage, using a gold disc working electrode (CH Instruments, Austin, TX, 0.02 cm^2 surface area), Ag/AgCl reference electrode and a Pt wire as an auxiliary electrode. The Cyclic voltammetry (CV) was utilized starting at the open circuit potential (OCP) to monitor the gold electrode modification using aqueous solutions of 1.0 M $NaClO_4$ containing 5.0 mM/5.0 mM $K_4[Fe(CN)_6]$/ $K_3[Fe(CN)_6]$ as the redox probe. Square wave voltammetry (SWV) and CV were employed to record the redox response of copper on the modified gold electrode using the 1.0 M $NaClO_4$ containing 10 mM phosphate buffer (pH 7.4) as an electrolyte. Gold electrodes were cleaned prior to each experiment by chemical, physical and electrochemical cleaning.[12] Briefly, piranha solution (H_2SO_4:H_2O_2 3:1 v/v) was used for chemical cleaning and then the gold electrodes were polishing with alumina slurry (0.1 µm and 0.05 µm for 2 min each) for physical cleaning followed by sonication in deionized water and anhydrous ethanol for 10 min. Electrochemical cleaning was performed utilizing CV (100 scans) in 0.5 M KOH and 0.5 M H_2SO_4 in the range of -2 to 0 and 0 to 1.5 volt, respectively. Electrodes were rinsed with deionized water after each step and were blown dried with compressed N_2 after final step.

The gold electrode modification was performed as previously described.[12,13] Briefly, cleaned gold electrodes were incubated in 2 mM Lip-NHS solution in ethanol at 4°C for 2 days followed by rinsing with ethanol and deionized water. Then, gold electrodes were immersed in 30 µM aqueous microtubule binding repeat R1-R4 solutions (pH 7.4) for 24 hours at 4°C. Modified gold electrodes were rinsed with deionized water followed by blown dried with N_2 flow. The modified electrodes were then incubated in 0.5 mM $Cu(ClO_4)_2$ solution for 1 hours at 25°C. The control experiments were performed by Cu^{2+} free gold electrode. The redox activity of Cu^{2+} in the R-Cu complex was monitored using 1.0 M $NaClO_4$ containing 10 mM phosphate buffer pH 7.4 as an electrolyte. Open circuit potential (OCP) of modified gold electrodes was recorded for 18 min in 0.5 mM ascorbic acid solution in order to monitor the redox activity of Cu^{2+} in Cu-R complexes in a reducing environment.

- **Transmission electron microscopy (TEM) experiment**

The TEM experiment were performed on a Hitachi H7500 transmission electron microscope using Olympus SIS MegaView II 1.35MB digital camera and iTEM version 5.2 software. For the TEM experiments, 1 mM aqueous tau peptides (R1-R4) solutions were incubated at pH 7.4 in a solution of a) 2 mM $CuCl_2$; b) 5 mM ascorbic acid and 0.5 mM $CuCl_2$; c) 2 mM of H_2O_2 d)2 mM $CuCl_2$ and 1mM glutathione in limited access of oxygen; e) 0.5 mM $CuCl_2$ and 10 mM glutathione; f) 0.5 mM $CuCl_2$, 10 mM glutathione and 10 mM ascorbic acid for 3 and/or 4 days at room temperature. The peptide solutions were diluted to 400 µM before taking the TEM image and aliquots of 5 µL were placed on carbon coated copper grids (CF300-Cu, Electron Microscopy Sciences). The grid was allowed to dry at room temperature. Then each grid was stained by adding 5 µL of aqueous uranyl acetate (2%) on it for 1 min. Excess solution was removed using the filter paper.

- **Electron paramagnetic resonance (EPR) spectroscopy**

EPR spectra were recorded using a X-band Bruker EMX spectrometer, operating at a microwave frequency 9.35 GHz with a microwave power of 2.1 mW. Magnetic field was swept from 2200 G to 3800 G, for detection 100 kHz field modulation was used with 1.0 G modulation amplitude. Experiments were carried out at 130 K using liquid nitrogen. The X-band EPR were collected from frozen samples after 16 scans. The EPRNMR software developed by Dr. Weil group (Mombourquette, M.J., Weil, J.A., and McGavin, D.G. (1996) EPR-NMR User's Manual, Department of Chemistry, University of Saskatchewan, Saskatoon, Canada) was used for data simulation. In order to interpret the data using Peisach-Blumberg plot[14,15], the $A_{\parallel}$ value was converted to A(milikaisers) using the following equation.

$A(mK)= 0.046686 \times g \times \Delta H$

Where g=2.0023 and ΔH is $A_{\parallel}$ (G)

The $CuCl_2$ solution was added to the microtubule binding repeats R1-R4 for the final concentration of 5 mM Cu^{2+} and 2.5 mM peptides in order to shift the equilibrium to the formation of R-Cu complex. All the solutions were kept at 25° C for 24 hours, and then diluted in the phosphate buffer, pH 7.4 right before the experiment to the final concentration of 1.8 mM and 0.9 mM for Cu^{2+} and peptides, respectively. A solution of 0.9 mM $CuCl_2$ was measured as control sample, which showed that the EPR signal for Cu^{2+} solution in phosphate buffer (pH 7.4) is negligible and does not interfere with the signal of the R-Cu complex. All the measurements carried on the frozen samples.

- **Gel electrophoresis**

The gel electrophoresis was performed on the 6.5% precast polyacrylamide gel using Mini-PROTEAN electrophoresis cells (Bio-Rad Laboratories (Canada Ltd.) and with starting voltage of 100 mV and 65 A. After 5 min voltage was decreased to 50 mV and kept for 90 min and then reduced to 40 mV. The 1 mM solution of each microtubule binding repeat was incubated with 2 mM $CuCl_2$ solution at 25° C for 24 hours. The 1 mM of each microtubule binding repeat solution without $CuCl_2$ solution was incubated at same condition as a control sample. After 24 hours, half of the Cu-R solution was incubated with the 2mM EDTA and 19 mg/mL (0.12 M) Dithiothreitol (DTT) for 2 hours at 30°C to cleave the disulfide bond. The 1 mM solution of microtubule bind repeat R2 and R3 were incubated in a mixture of 10 mM ascorbic acid and 0.5 mM $CuCl_2$ for 2 hours at room temperature in order to evaluate the impact of Cu^{2+} in reducing environment. The 1 mM solution of R2/R3 were incubated for 2 hours at room temperature in 2 mM H_2O_2 in order to evaluate the disulfide bond formation with different redox agent. As control samples 1 mM R2/R3 were incubated at the same condition with and without 2 mM $CuCl_2$. After 2 hours, half of the Cu-R solution was incubated with the 2mM EDTA and 19 mg/mL DTT for 2 hours at 30°C to cleave the disulfide bond. To evaluate the effect of glutathione on the dimerization of R2 and R3, 1 mM of the peptides were incubated in a) 2 mM $CuCl_2$ and 1mM glutathione in limited access of oxygen; b) 0.5 mM $CuCl_2$ and 10 mM glutathione; c) 0.5 mM $CuCl_2$,10 mM glutathione and 10 mM ascorbic acid.

All the samples were diluted in tricine sample buffer containing 200 mM Tris-HCl, pH 6.8, 40% glycerol, 2% SDS, 0.04% Coomassie Blue G-250 and 0.5 µg of each samples were loaded to the gel. The 10x premixed electrophoresis buffer, contains 100 mM Tris, 100 mM Tricine, 0.1% SDS, pH 8.3 following 10 times dilution with water was used as running buffer. The standard protein of Precision Plus Protein™ Dual Xtra Prestained Protein Standards, which is the mixture of 12 recombinant proteins (2–250 kD) was run as well for determining the mass of peptides bonds.

- **Dynamic Light Scattering**

The dynamic light scattering (DLS) experiments were performed at Zetasizer Nano ZSP (Malvern Instrument, UK). All the measurements were carried out at the control temperature of 25^{o}C. An average of 3 measurements were used for the calculation using Zetasizer Software. 1 mM aqueous solutions of R2 and R3 were incubated at pH 7.4 in 2 mM $CuCl_2$ solution for 4 days at room temperature. Samples diluted to the final concentration of 0.2 mM of R2/R3 prior to analysis.

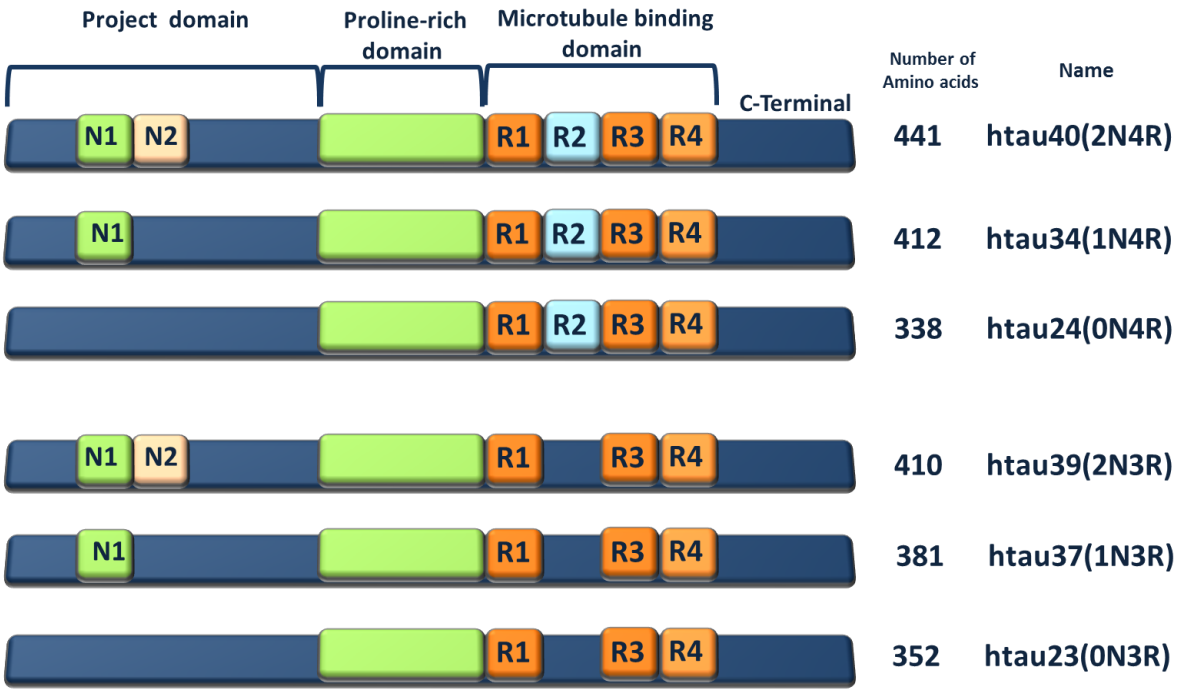

Scheme S1. Schematic presentation of the six tau protein isoforms in the human brain. The name and the number of amino acids of each isoform is showed at the right (htau40, htau34, htau24, htau39, htau37 and htau23). The major domain of each isoform is showed in the left, which consist of project domain, proline-rich domain and microtubule binding domain. The tau isoforms can be characterized based on the number of microtubule binding repeats; htau40, htau34, and htau24 have four microtubule binding repeats, while htau39, htau37 and htau23 only have three microtubule binding repeats including R1, R3 and R4.

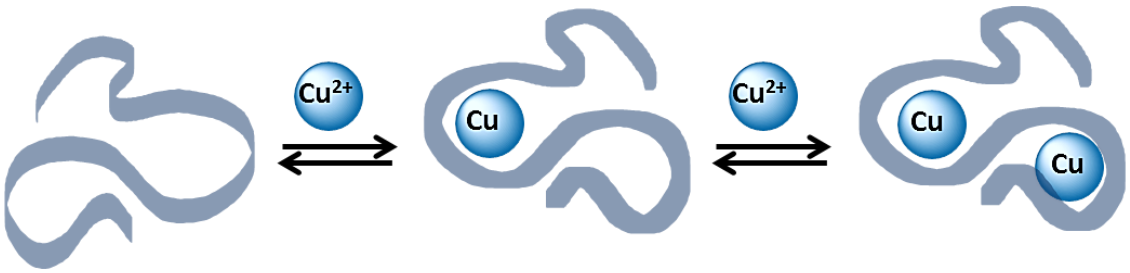

Scheme S2. Schematic representation of the hypothetical two-step reaction of the Cu^{2+}-peptide complexation.

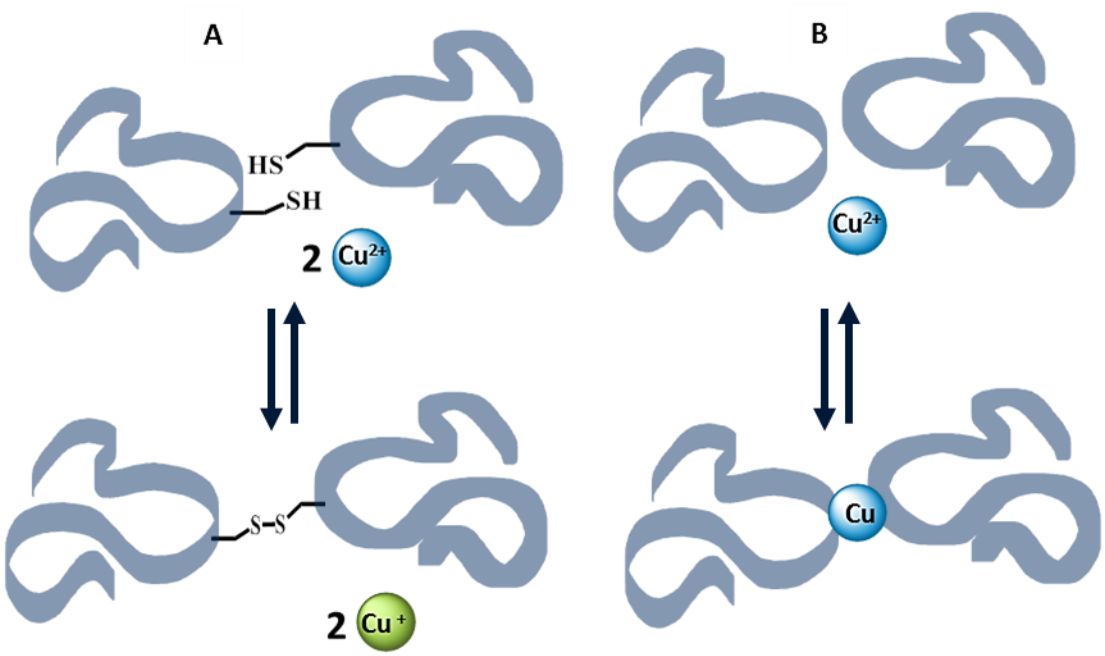

Scheme S3. Schematic representation of the two possible pathways for mediation of Cu^{2+} in R2 and R3 dimerization. (A) Cu^{2+} trigger the peptide dimerization by oxidizing the cysteine to cystine to form the disulfide bond. (B) Cu^{2+} coordinate to amino acids of two monomers and make a bridge to form a dimer.

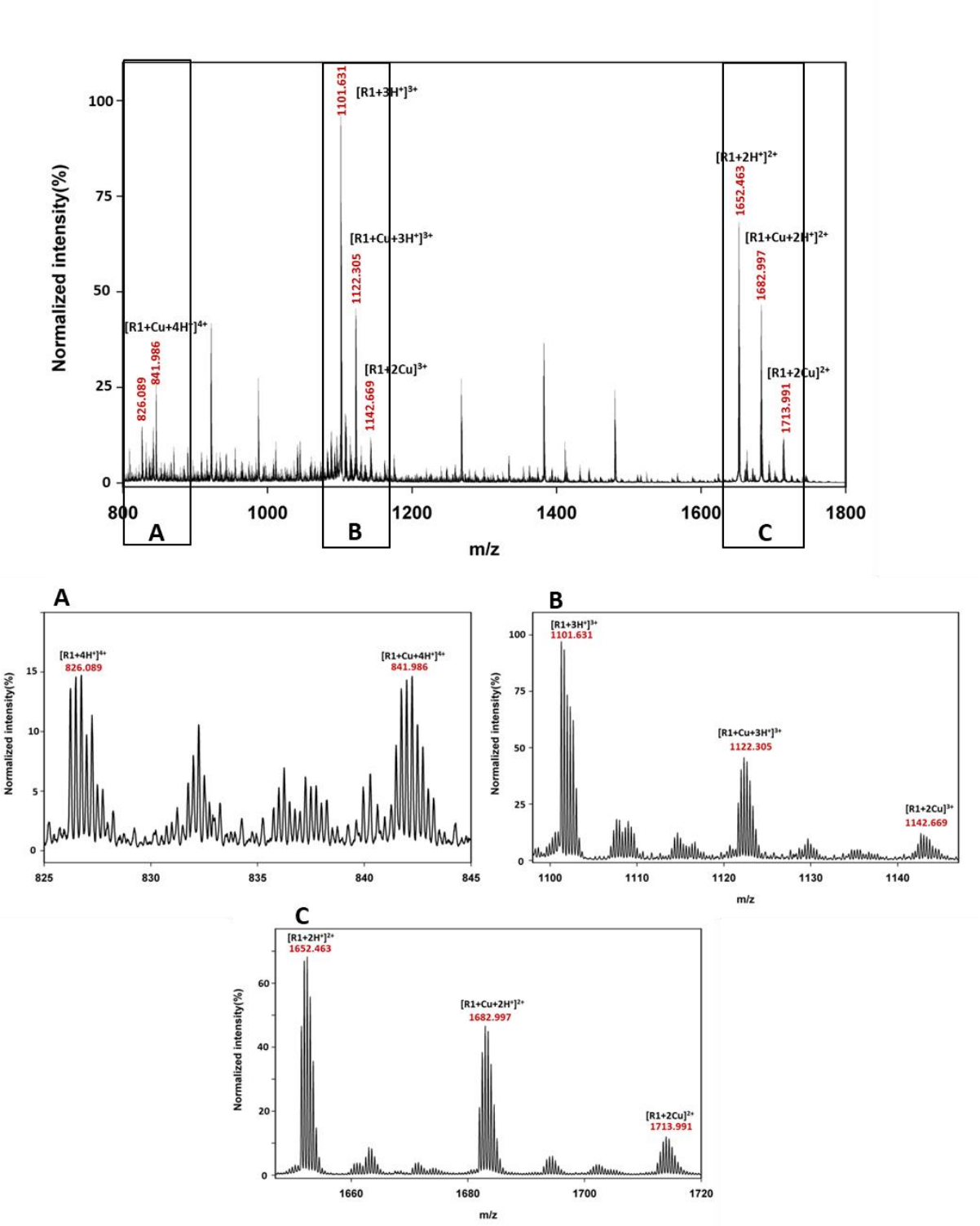

Figure S1. The ESI-MS spectra together with isotope pattern (A, B, and C) of microtubule binding repeat R1 after incubating in Cu^{2+} (1:2 molar ratio of R:Cu at 70 µM of R) solution at 25°C (pH 7.4) for 24 hours. The ESI-MS spectrum confirms the mono and di metallation of R1 after incubation in Cu^{2+} solution.

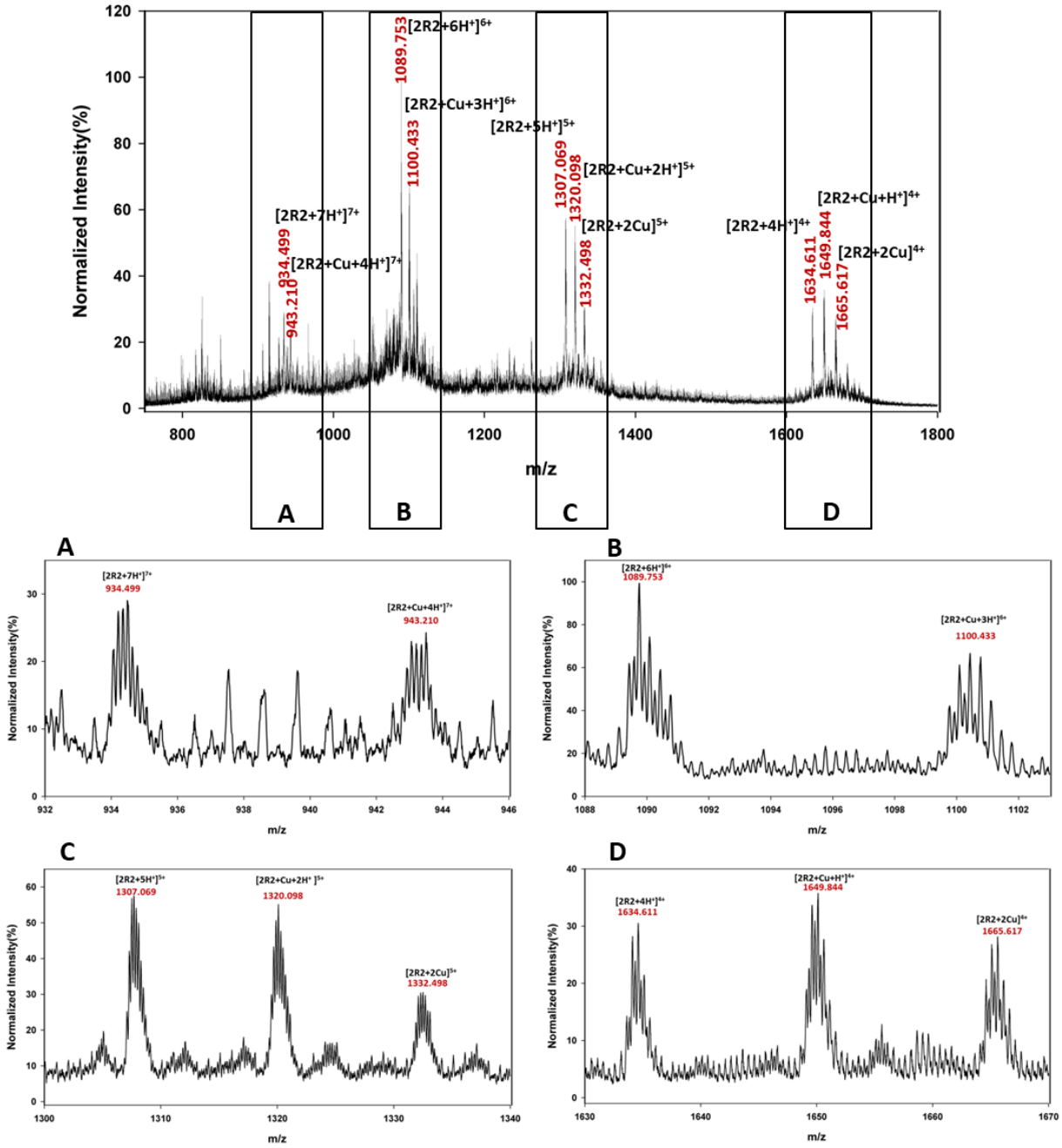

Figure S2. The ESI-MS spectra together with isotope pattern (A, B, C, and D) of microtubule binding repeat R2 after incubating in Cu^{2+} (1:2 molar ratio of R:Cu at 70 µM of R) solution at 25°C (pH 7.4) for 24 hours. The ESI-MS experiment confirms the dimer formation as well as mono and dimetallation of R2 dimers after incubation in Cu^{2+} solution.

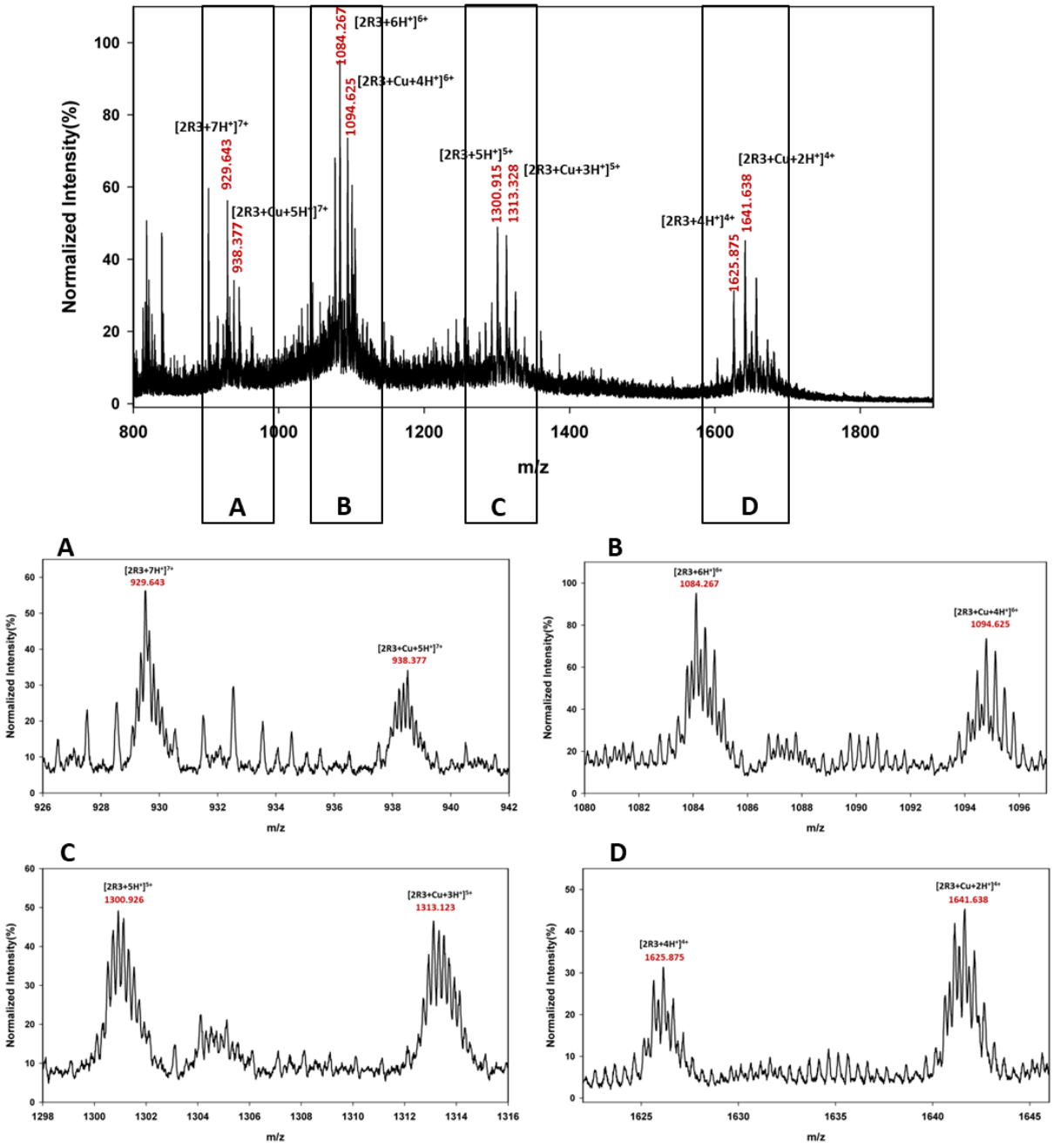

Figure S3. The ESI-MS spectra together with isotope pattern (A, B, C and D) of microtubule binding repeat R3 after incubating with Cu^{2+} (1:2 molar ratio of R:Cu at 70 µM of R) solution at 25°C (pH 7.4) for 24 hours. The ESI-MS experiment confirms the dimer formation as well as mono metallation of R3 dimers after incubation in Cu^{2+} solution.

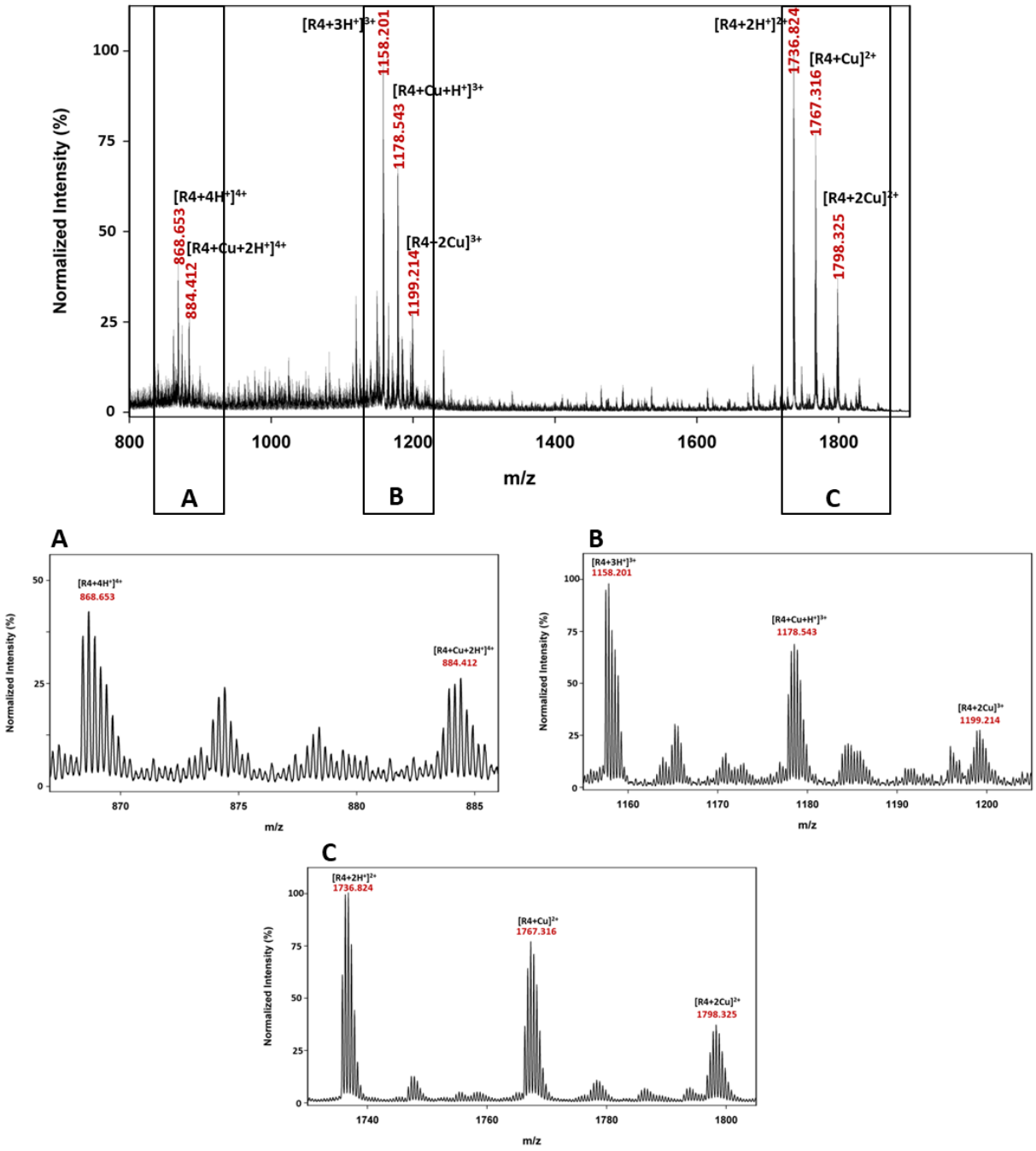

Figure S4. The ESI-MS spectra together with isotope pattern (A, B, and C) of microtubule binding repeat R4 after incubating with Cu^{2+} (1:2 molar ratio of R:Cu at 70 µM of R) solution at 25°C (pH 7.4) for 24 hours. The ESI-MS spectrum confirms the mono and dimetallation of R4 after incubation in Cu^{2+} solution.

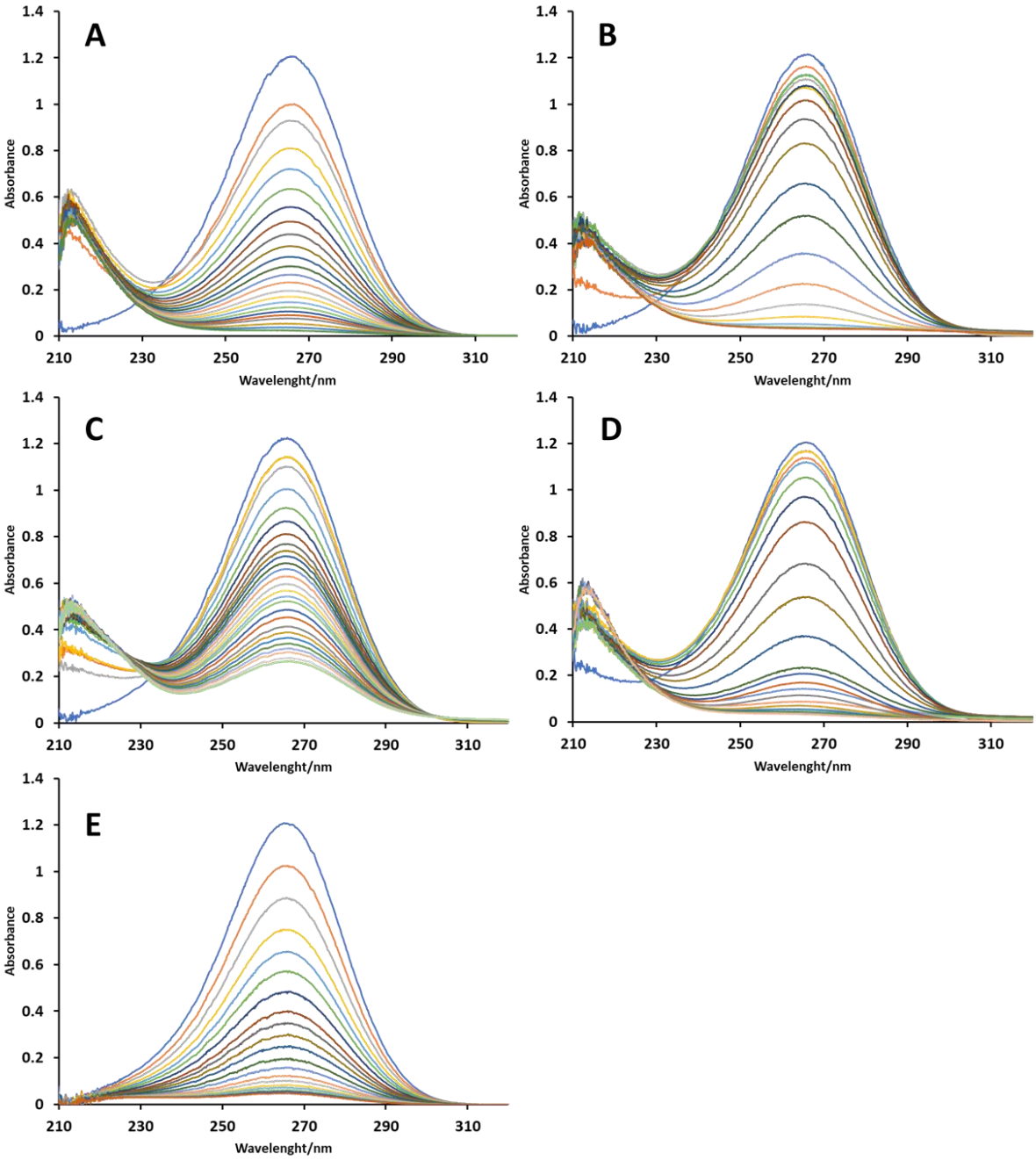

Figure S5. Probing the redox activity of Cu-R complexes in presence of 100 µM ascorbic acid (AA). UV-vis spectrum of ascorbic acid at different time intervals in the solution of (A) Cu-R1 for 20 min, (B) Cu-R2 for 50 min, (C) Cu-R3 for 120 min, (D) Cu-R4 for 20 min complexes (molar ratio of 10:2:1 for AA:R:Cu) and (E) control experiments using $CuCl_2$ without peptide for 20 min. The Reaction was monitored until no changes in absorbance observed.

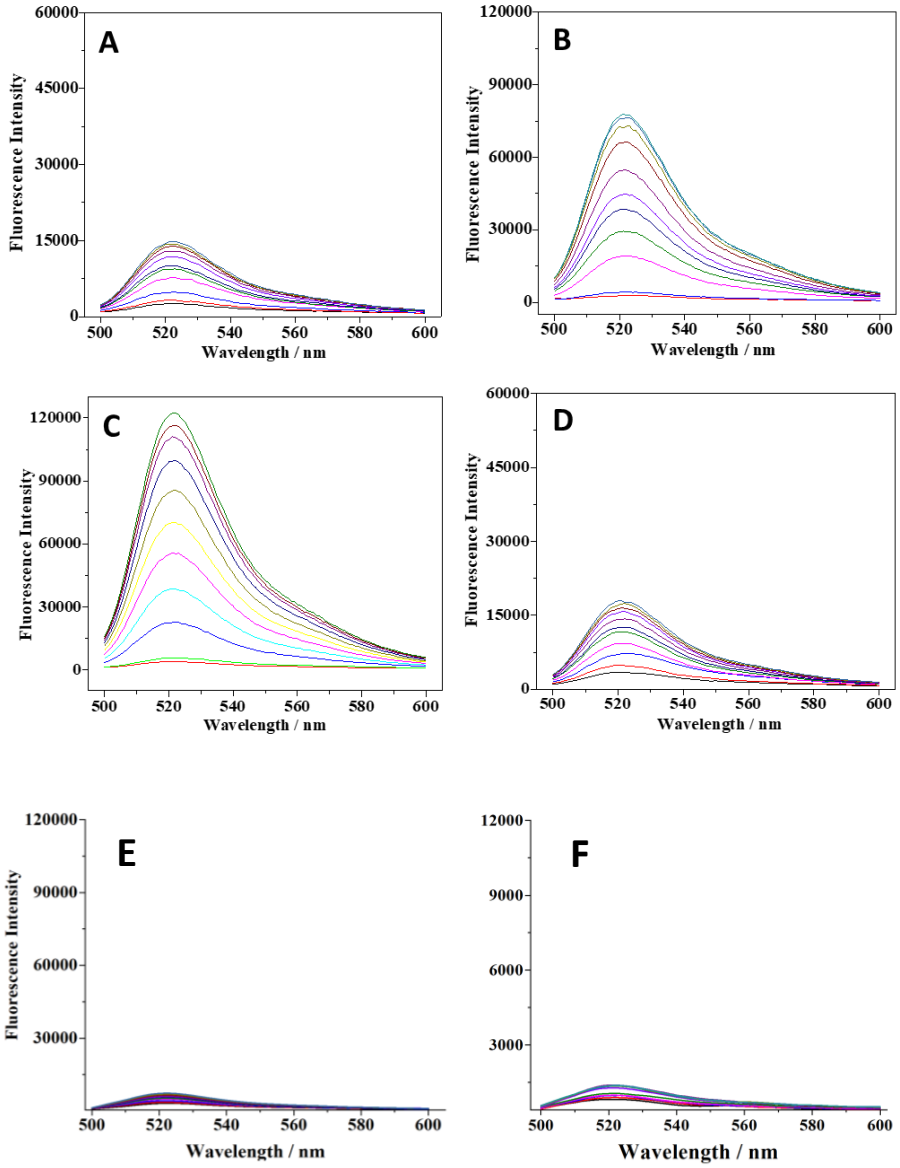

Figure S6. Time dependent study of the formation of reactive oxygen species (ROS) due to interactions of Cu^{2+} with microtubule binding repeats R1-R4. Fluorescence spectra of 2,7-dichlorofluorescein (DCF) in the presence of 5 µM Cu^{2+} solution with (A) R1, (B)R2, (C)R3 and (D) R4 (2:1 molar ratio of Cu: R) at different time intervals. Samples were scanned every 10 min for total session of 120 min. (E) and (F) fluorescence spectrum for the control experiment of DCF with Cu^{2+} (E) and GSH with Cu^{2+} (F).

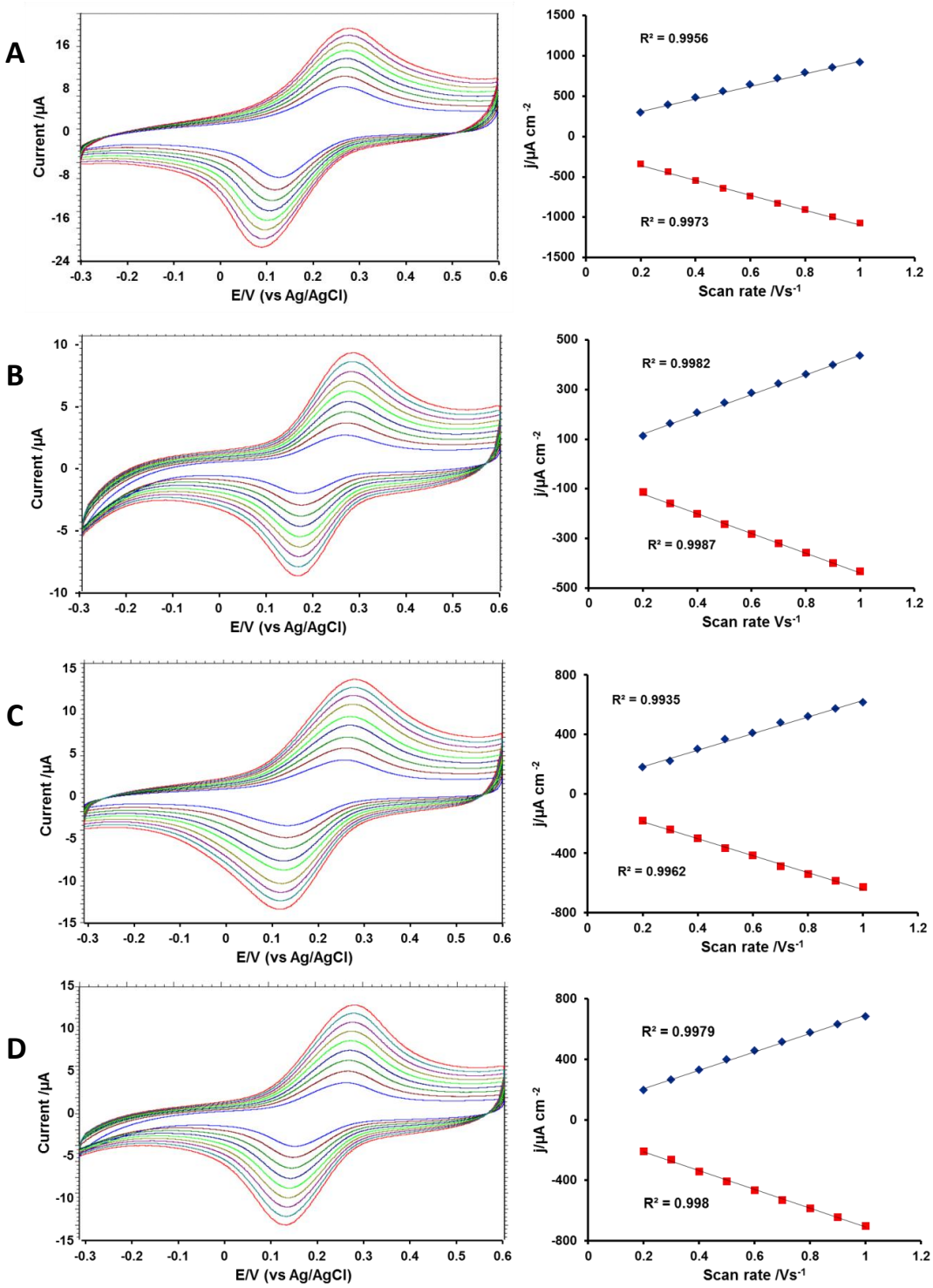

Figure S7. Influence of the scan rate on the copper electrochemical response of modified gold electrode after incubating in 0.5 mM Cu^{2+} solution. Cyclic voltamogramm of gold modified electrode (left) with A)R1, B)R2, C)R3 and D)R4 after incubating in Cu^{2+} solutions for one hour at room temperature (scan rate: 0.2-1 V S^{-1}) . Plot of peak current density vs the scan rate (right) of the copper oxidation and reduction signals of modified gold electrode with A) R1, B) R2, C) R3 and D) R4 after incubating in 0.5 mM Cu^{2+} solution.

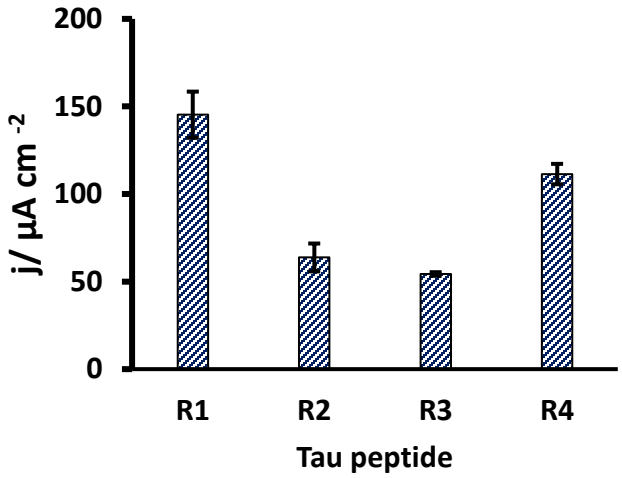

Figure S8. Plot of the current densities of copper redox response of the modified gold electrode (modified with R1,R2,R3 and R4) after incubating in 0.5 mM Cu^{2+} solution. Current densities were taken from square wave voltammograms (SWV) in 10 mM phosphate buffer (pH 7.4). Ag/AgCl as a reference electrode and Pt wire as a counter-electrode). Error bars show the standard deviation of triplicate measurements.

Table S1. Copper oxidation potential of the modified gold electrode with R1, R2, R3, and R4 after incubating in 0.5 mM Cu^{2+} solution, obtaining from SWV in 10 mM phosphate buffer (pH 7.4). (Ag/AgCl as a reference electrode and Pt wire as a counter-electrode).

	R1	**R2**	**R3**	**R4**
E/mV (SWV)	212±7	176±1	176±6	184±4

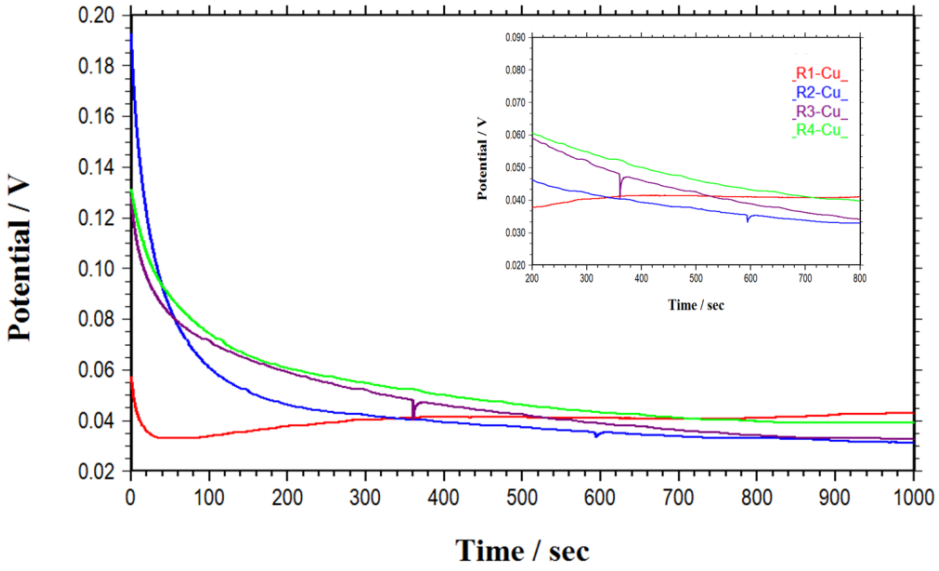

Figure S9. Probing redox activity of Cu^{2+} on Cu-R film. Plot of open circuit potential (OCP) vs time of modified gold electrode with microtubule binding repeat R1 (red), R2 (blue), R3 (purple) and R4 (green) after incubating in Cu^{2+} solution in 0.5 mM ascorbic acid solution as electrolyte, Ag/AgCl as a reference electrode and Pt wire as a counter-electrode.

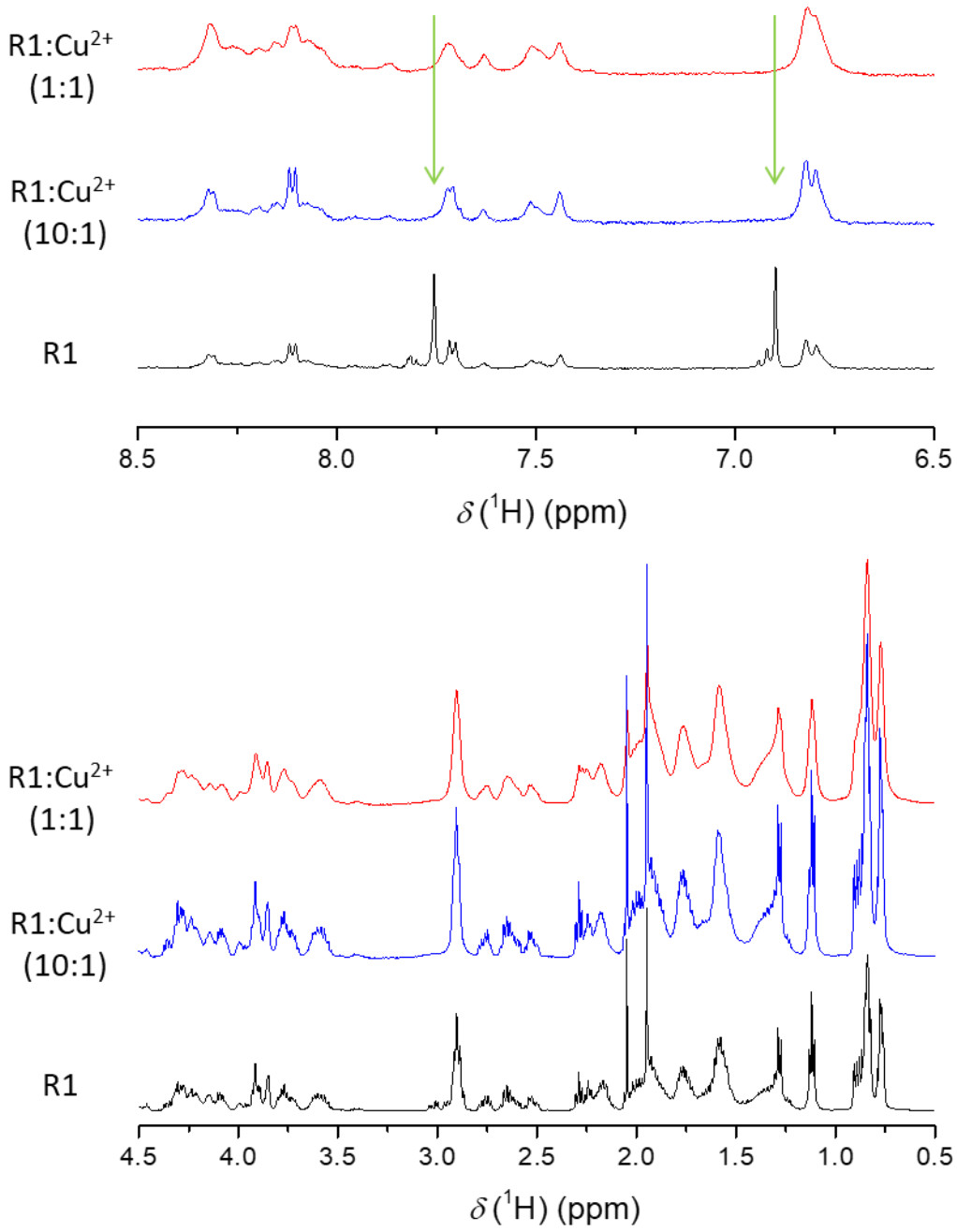

Figure S10. ^{1}H NMR spectra (aromatic region, upper panel and aliphatic region, lower panel) for 2 mM microtubule binding repeat R1 (black), R1 after incubating in Cu^{2+} solution at 25°C (pH 7.4) with molar ratio of 10:1 (blue) and 1:1 (red) peptide to copper. Peaks at 6.9 and 7.7 ppm, which are belong to imidazole ring of histidine, disappeared after incubation in Cu^{2+} solution due to paramagnetic effect. These results confirm that the histidine is the binding site of copper.

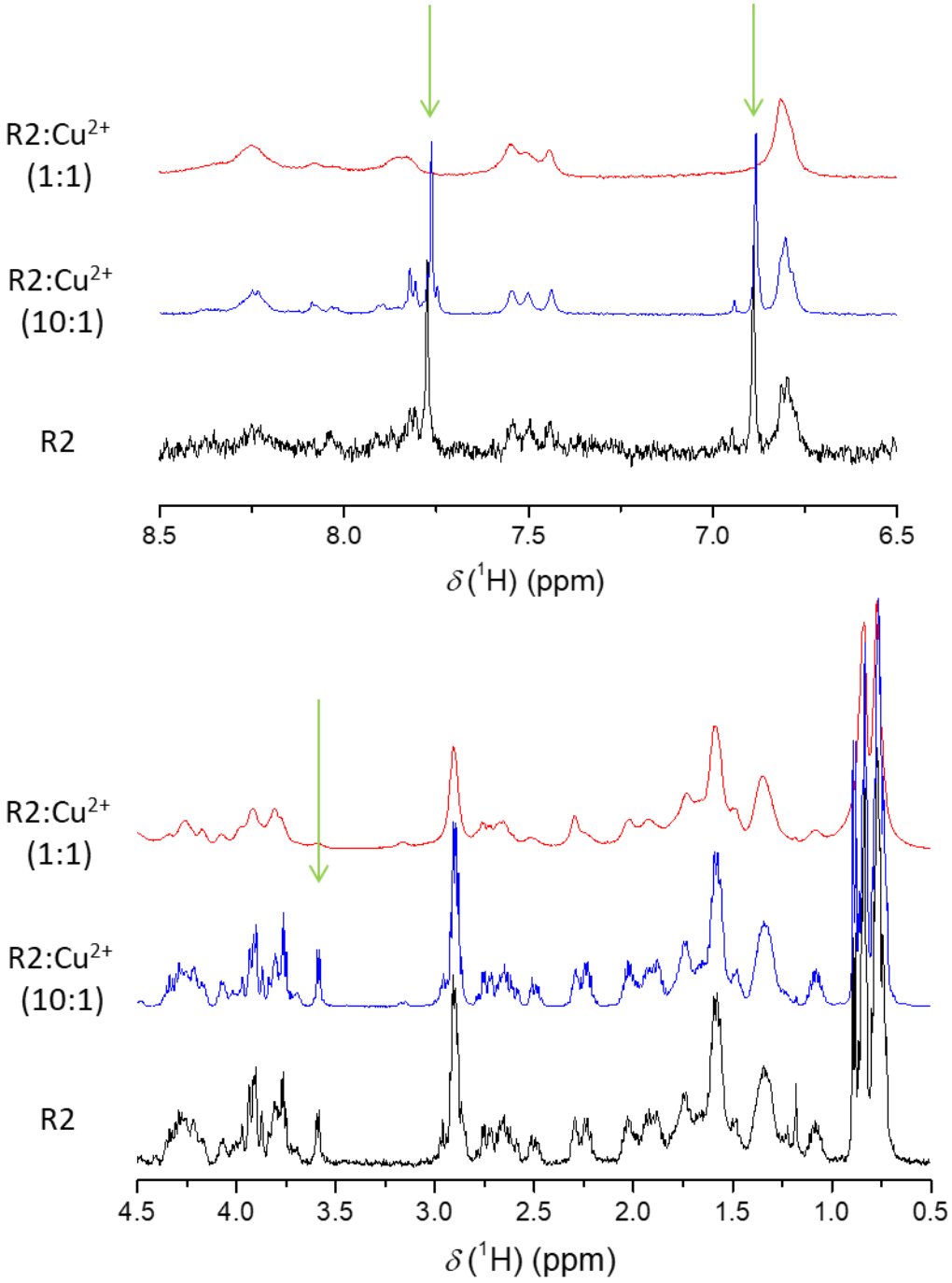

Figure S11. ^{1}H NMR spectra (aromatic region, upper panel and aliphatic region, lower panel) for 2 mM microtubule binding repeat R2 (black), R2 after incubating in Cu^{2+} solution at 25°C (pH 7.4) with molar ratio of 10:1 (blue) and 1:1 (red) peptide to copper. Peaks at 6.9 and 7.7 ppm, which are belong to imidazole ring of histidine, disappeared after incubation in Cu^{2+} solution due to paramagnetic effect. These results confirm that the histidine is the binding site of copper. In the aliphatic region, disappearing of peak at 3.6 ppm, which is belong to the cysteine, indicates the involvement of the cysteine in Cu-R2 interaction.

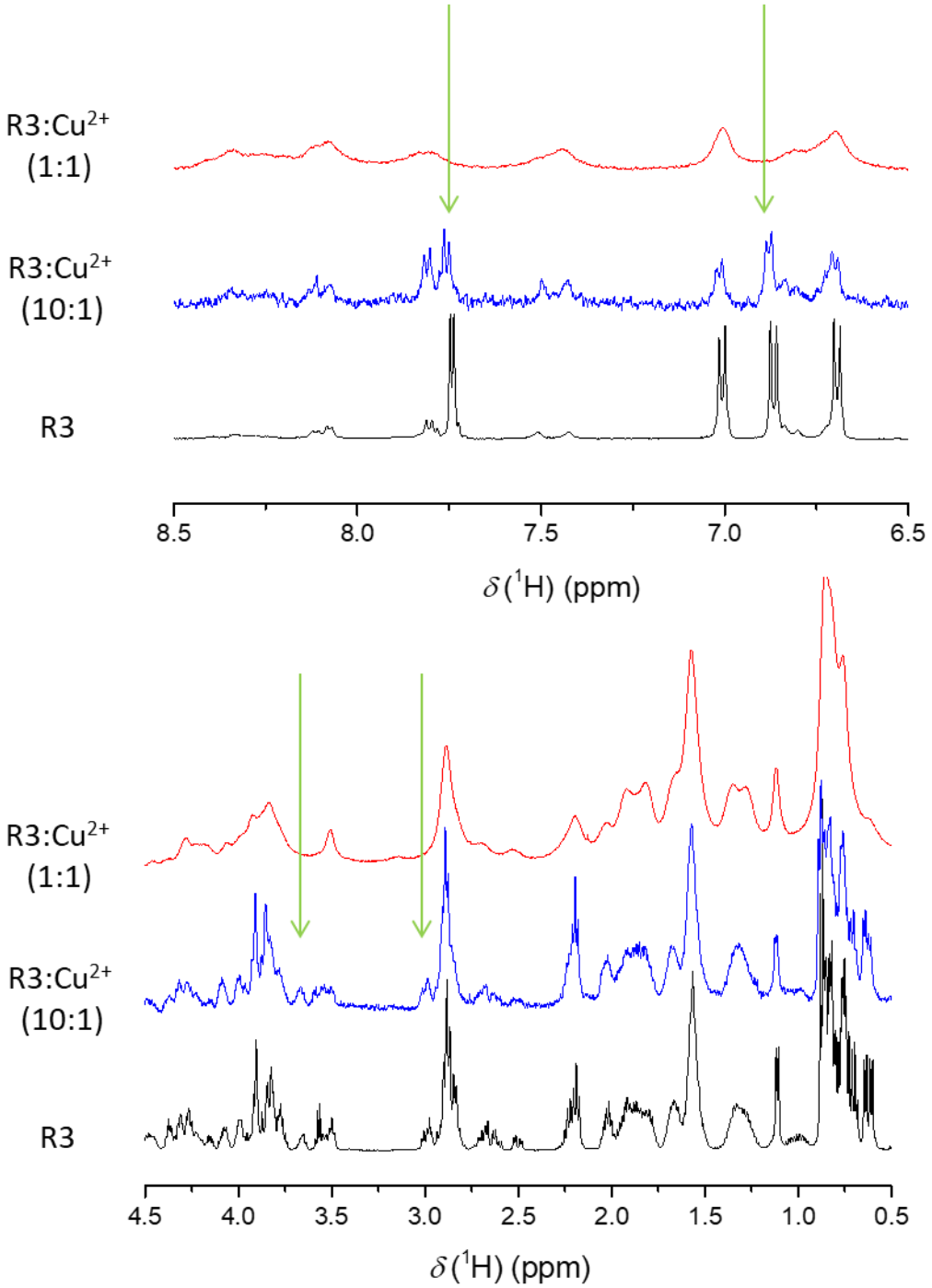

Figure S12. ^{1}H NMR spectra (aromatic region, upper panel and aliphatic region, lower panel) for 2 mM microtubule binding repeat R3 (black), R3 after incubating in Cu^{2+} solution at 25°C (pH 7.4) with molar ratio of 10:1 (blue) and 1:1 (red) peptide to copper. Peaks at 6.9 and 7.7 ppm, which are belong to imidazole ring of histidine, disappeared after incubation in Cu^{2+} solution due to paramagnetic effect. These results confirm that the histidine is the binding site of copper. In the aliphatic region, disappearing of peaks at 3 and 3.6 ppm, which is belong to the cysteine, indicates the involvement of the cysteine in Cu-R3 interaction.

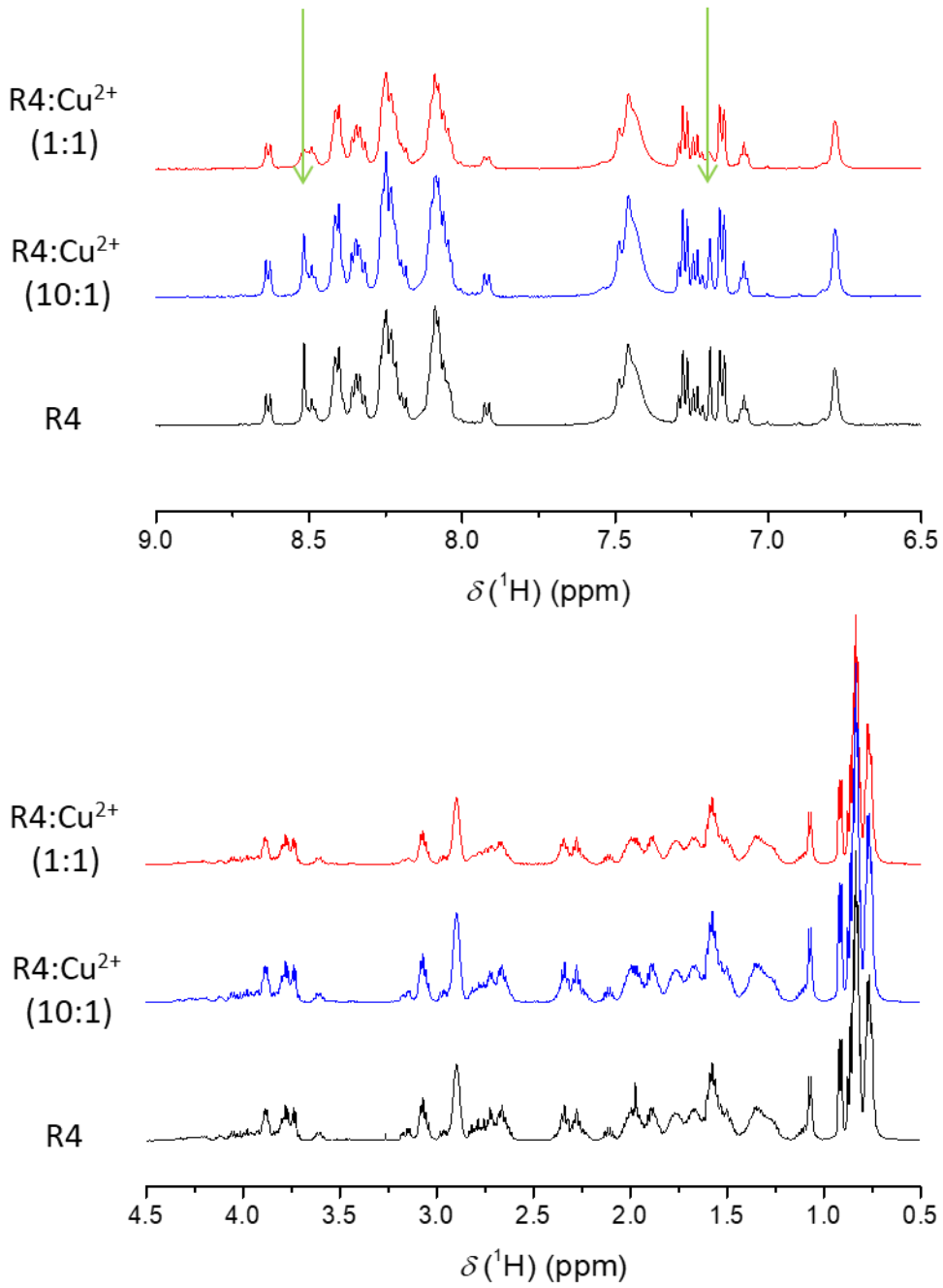

Figure S13. ^{1}H NMR spectra (aromatic region, upper panel and aliphatic region, lower panel) for 2 mM microtubule bind repeat R4 (black), R4 after incubating in Cu^{2+} solution at 25°C (pH 7.4) with molar ratio of 10:1 (blue) and 1:1 (red) peptide to copper. Peaks at 7.2 and 8.5 ppm, which are belong to imidazole ring of histidine, disappeared after incubation in Cu^{2+} solution due to paramagnetic effect. These results confirm that the histidine is the binding site of copper.

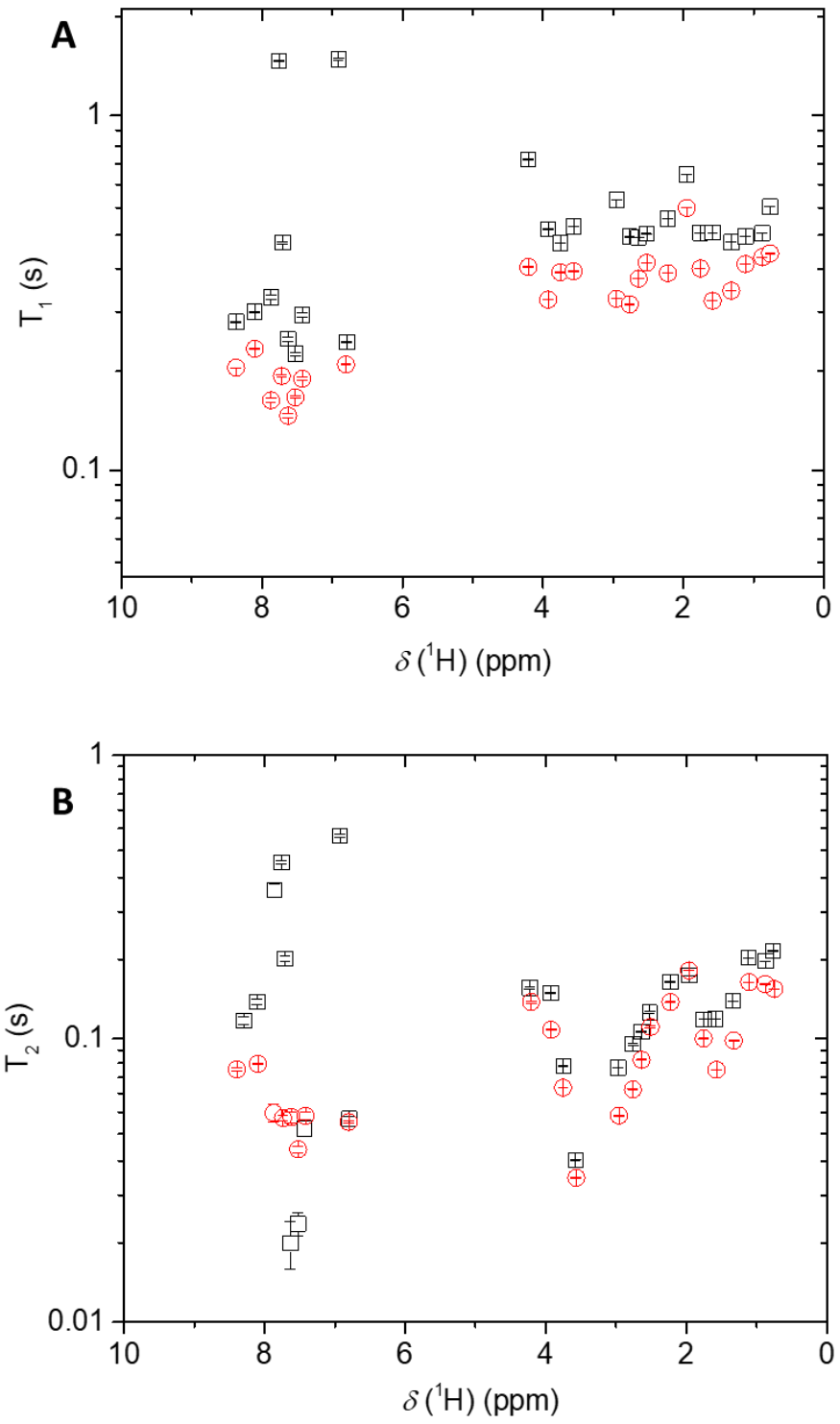

Figure S14. ^{1}H NMR T_1 plot (A) and T_2 plot (B) for 2 mM microtubule binding repeat R1 (black dots) and R1 after incubating in Cu^{2+} solution at 25°C (pH 7.4) with molar ratio of 1:1 (red dots). Significant changes in T_1 and T_2 in aromatic region is due to paramagnetic effect upon copper coordination.

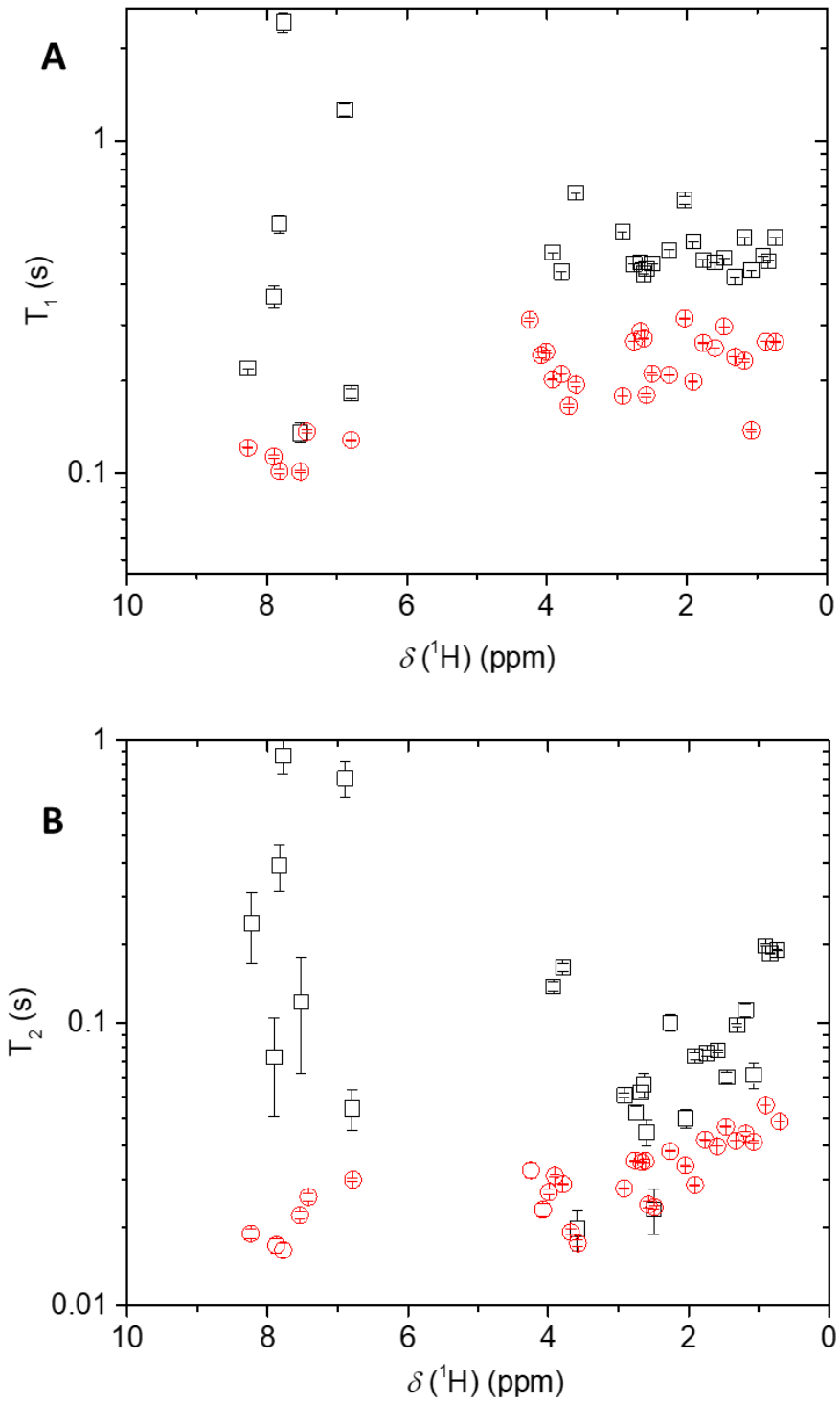

Figure S15. ^{1}H NMR T_1 plot (A) and T_2 plot (B) for2 mM microtubule binding repeat R2 (black dots) and R2 after incubating in Cu^{2+} solution at 25°C (pH 7.4) with molar ratio of 1:1 (red dots). Significant changes in T_1 and T_2 for all peaks presumably is due to aggregation upon copper interactions.

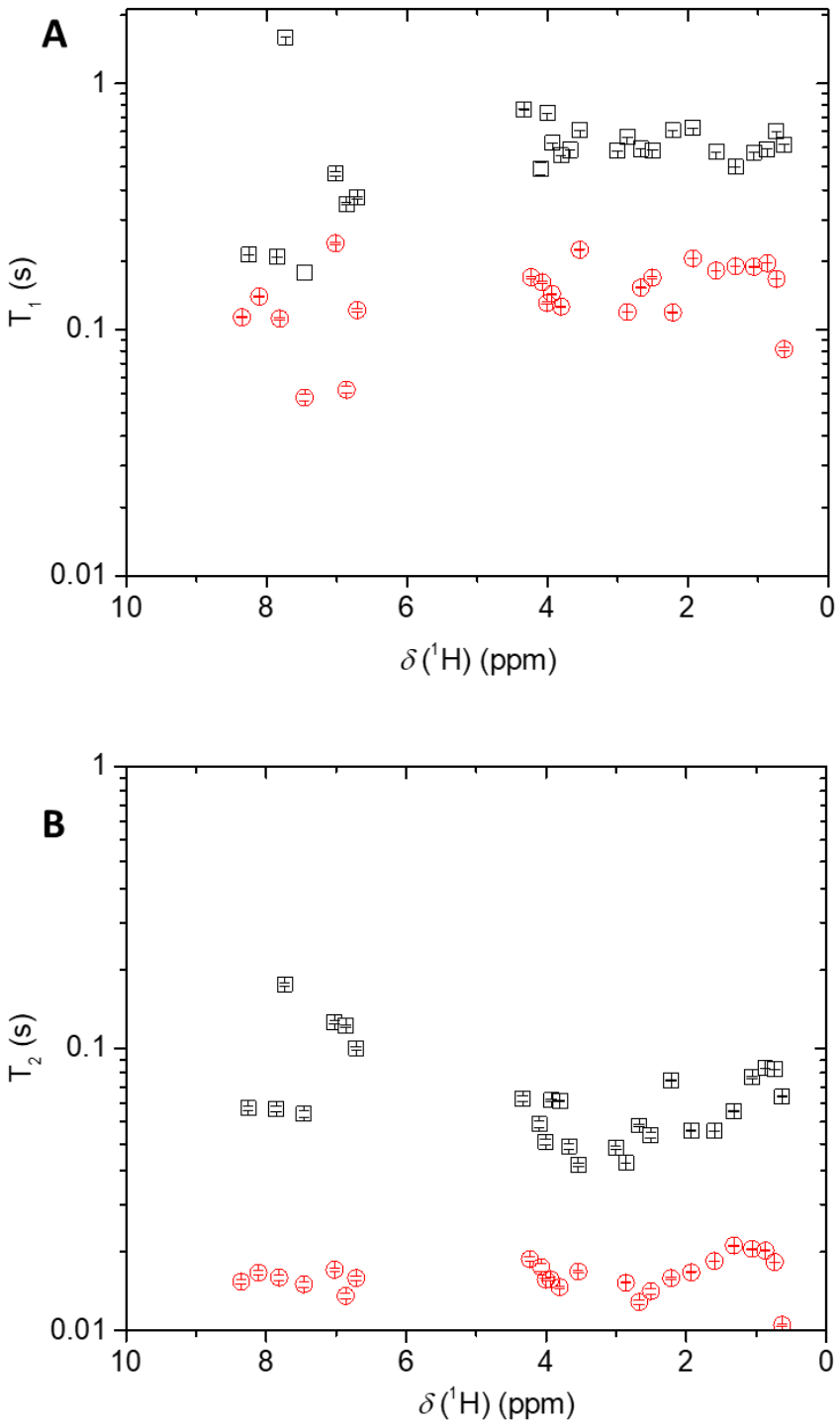

Figure S16. ^{1}H NMR T_1 plot (A) and T_2 plot (B) for 2 mM microtubule binding repeat R3 (black dots) and R3 after incubating in Cu^{2+} solution at 25°C (pH 7.4) with molar ratio of 1:1 (red dots). Significant changes in T_1 and T_2 for all peaks presumably is due to aggregation upon copper interaction.

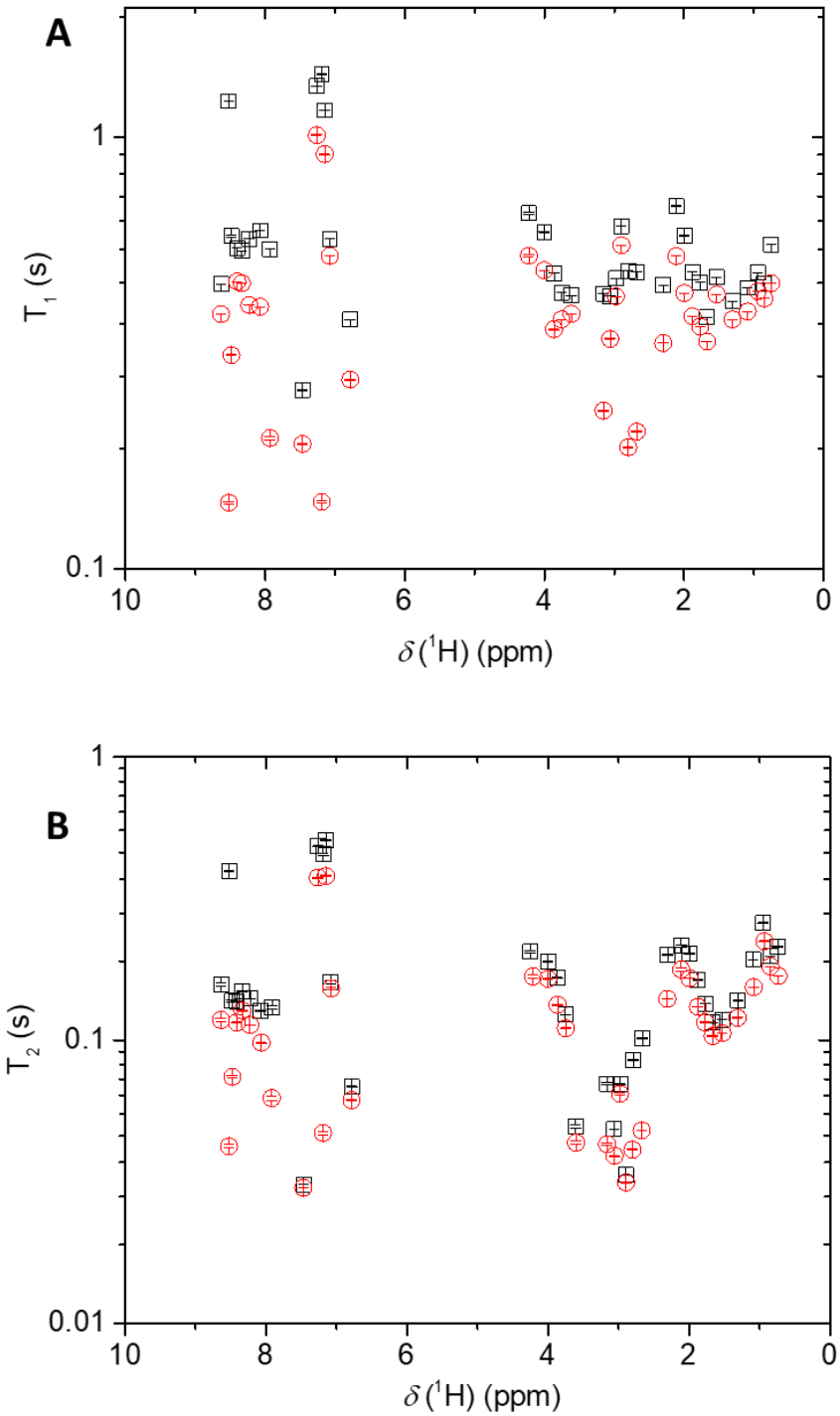

Figure S17. ^{1}H NMR T_1 plot (A) and T_2 plot (B) for 2 mM microtubule binding repeat R4 (black dots) and R4 after incubating in Cu^{2+} solution at 25°C (pH 7.4) with molar ratio of 1:1(red dots). Significant changes in T_1 and T_2 in aromatic region is due to paramagnetic effect upon copper coordination.

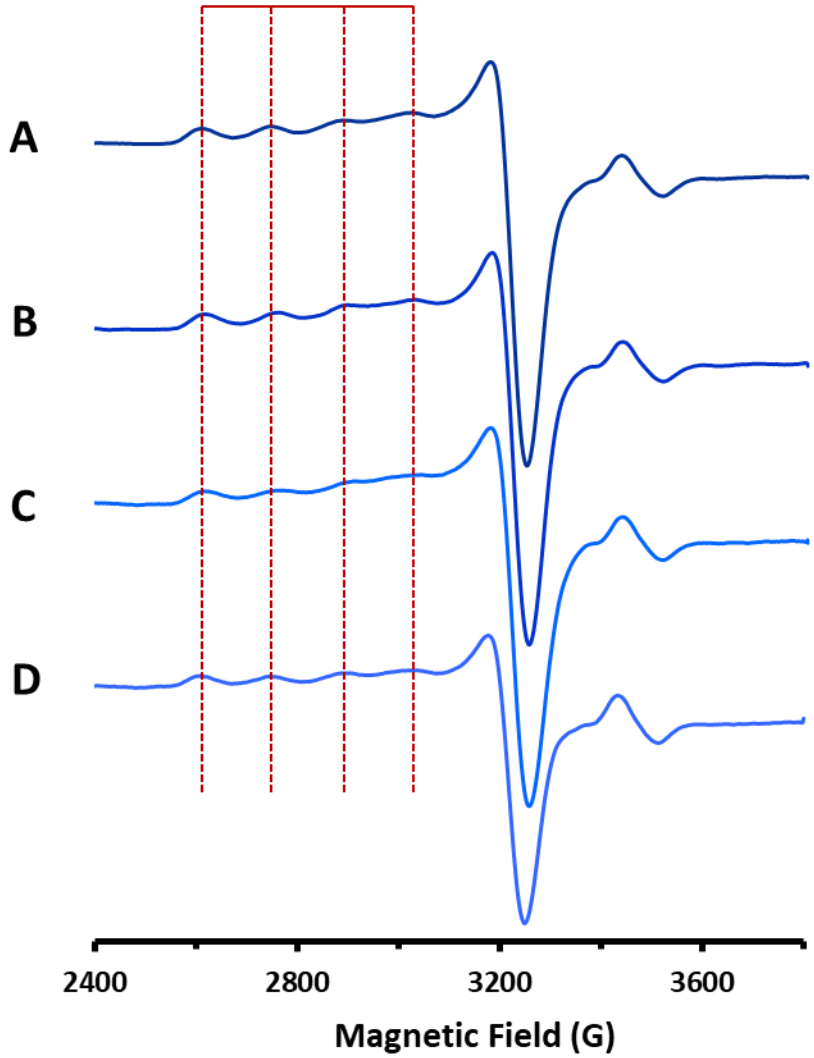

Figure S18. X-band EPR spectra of frozen solution of microtubule binding repeat A) R1, B) R2, C) R3 and D) R4 after incubating in Cu^{2+} solution at 25°C (pH 7.4) for 24 hours with molar ratio R:Cu of 1:2. The results confirm that all R-Cu complexes have the same coordination. The simulation gave the value of $g_{\parallel} = 2.361$ and $g_{\perp} = 2.077$, and hyperfine splitting $A_{\parallel} = 165$ G and $A_{\perp}$ equal to 9 G. Based on the Peisach-Blumberg classification, potential ligating sites include the His imidazole N (confirming by NMR), backbone amides N or O as well as other oxygen-based ligating sites, including potential influence of solvation. A suggested model is provided in Figure 4C.

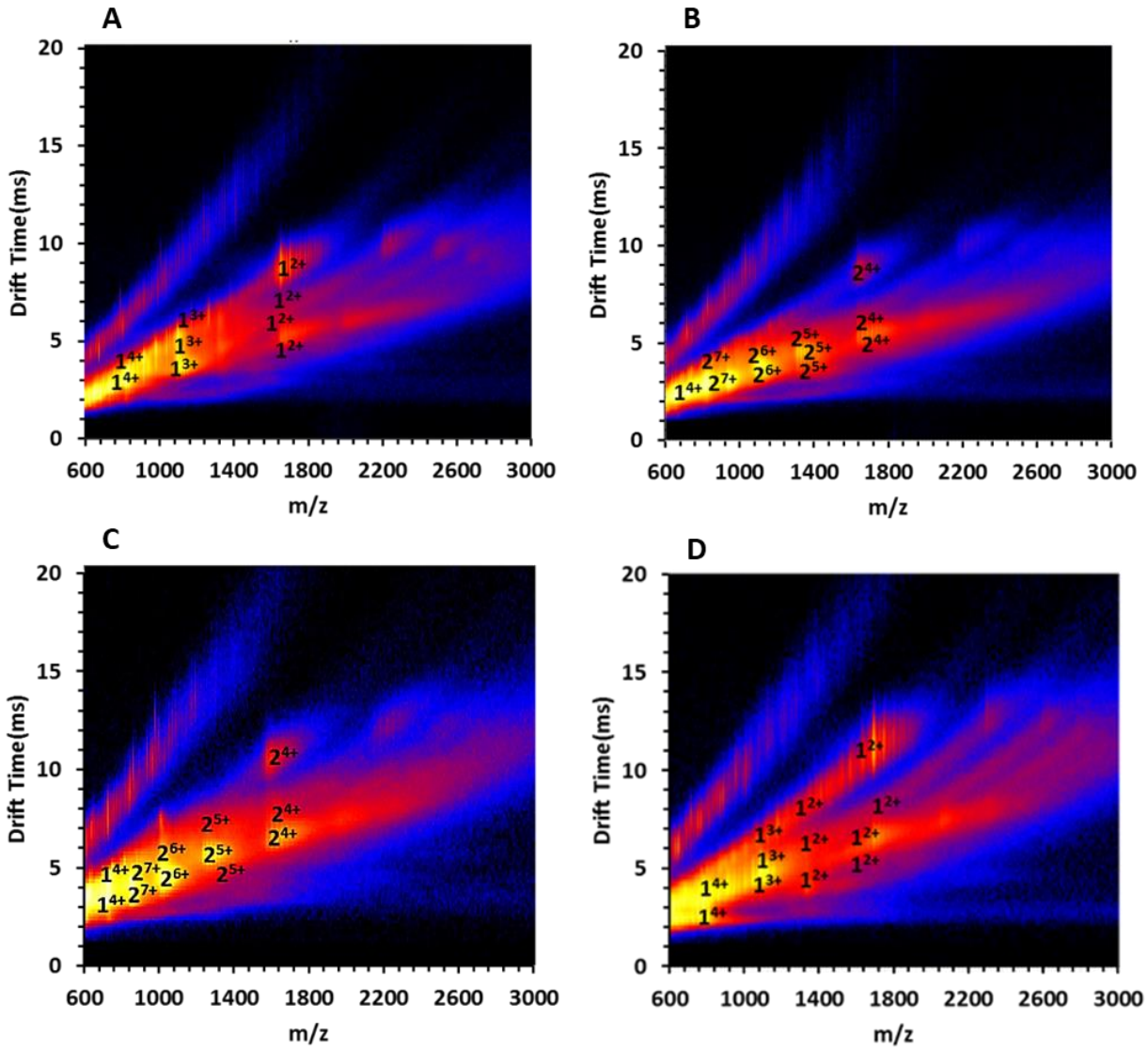

Figure S19. IMS-MS Driftscope plots (See Figure S21-S30 for drift time distribution plots) of microtubule binding repeats (A) R1, (B) R2, (C) R3 and (D) R4 after incubating in Cu^{2+} solution (2:1 molar ratio of Cu:R; 70 µM of R) at 25°C (pH 7.4) for 24 hours. The numbers on the Driftscope plots indicate monomer or dimer ions present and the adjacent superscript numbers show the charge states of those ions.

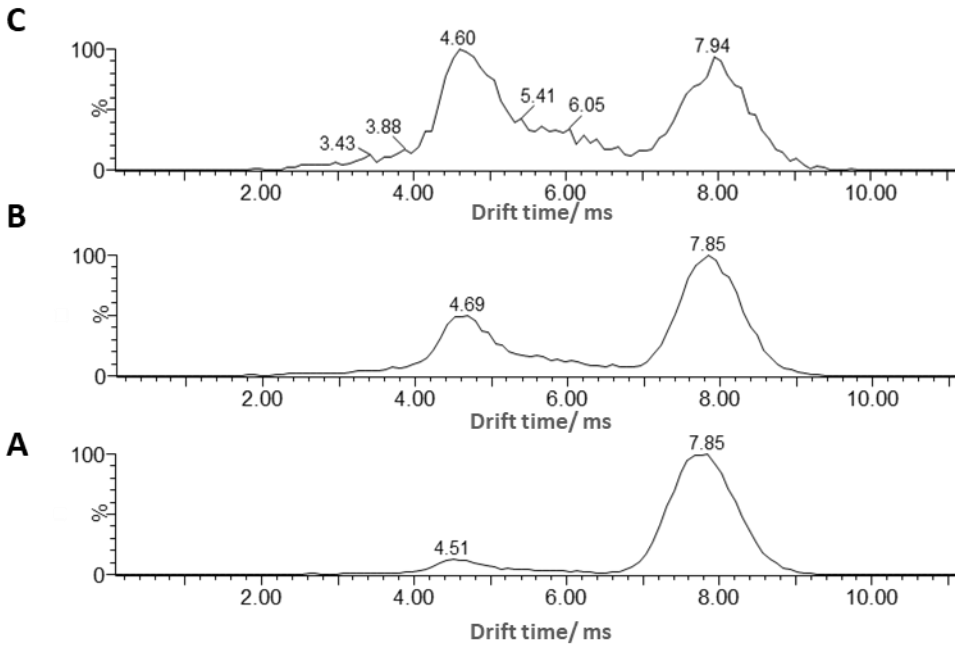

Figure S20. Drift time distribution as determined by ESI-IMS-MS for m/z corresponded to (A) $[R1+2H]^{2+}$, (B) $[R1+Cu+2H]^{2+}$ and (C) $[R1+2Cu]^{2+}$ (2:1 molar ratio of Cu:R; 70 µM of R). The enhancement of population with lower drift time for the $[R1+Cu+2H]^{2+}$ and $[R1+2Cu]^{2+}$ suggested that the Cu^{2+} trigger the conformational changes in R1.

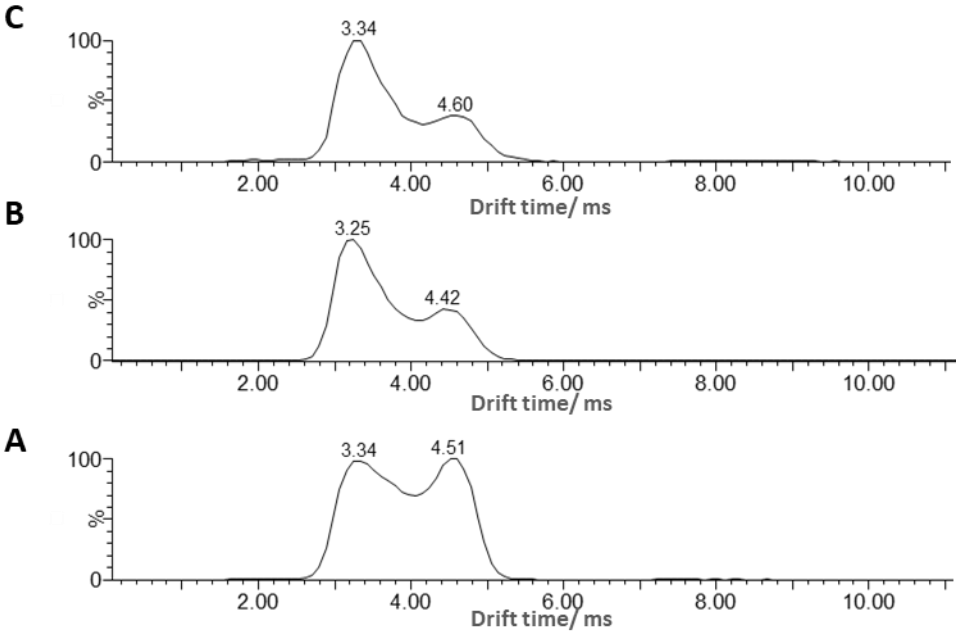

Figure S21. Drift time distribution as determined by ESI-IMS-MS for m/z corresponded to (A) $[R1+3H]^{3+}$, (B) $[R1+Cu+3H]^{3+}$ and (C) $[R1+2Cu]^{3+}$ (2:1 molar ratio of Cu:R; 70 µM of R). The enhancement of population with higher drift time for the $[R1+Cu+3H]^{3+}$ and $[R1+2Cu]^{3+}$ suggested that the Cu^{2+} trigger the conformational changes in R1.

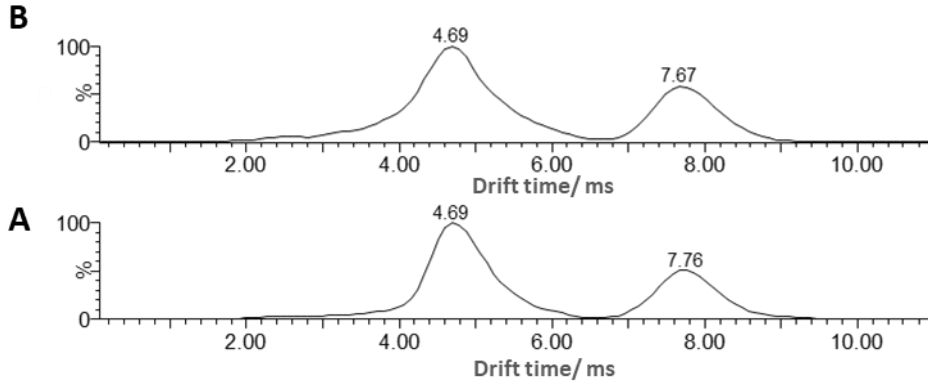

Figure S22. Drift time distribution as determined by ESI-IMS-MS for m/z corresponded to (A) $[2R2+4H]^{4+}$ and (B) $[2R2+Cu+H]^{4+}$ (2:1 molar ratio of Cu:R; 70 µM of R). The drift time remained unchanged upon copper coordination, which indicates that both R2 dimer with and without copper coordination has relatively similar collision cross section.

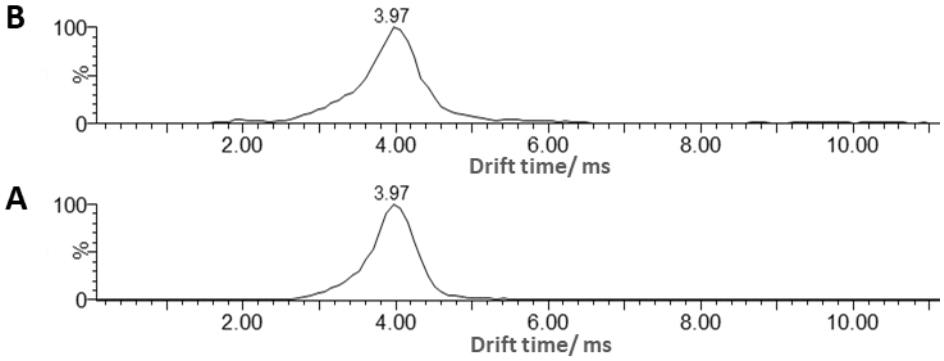

Figure S23. Drift time distribution as determined by ESI-IMS-MS for m/z corresponded to (A) $[2R2+5H]^{5+}$ and (B) $[2R2+Cu+2H]^{5+}$ (2:1 molar ratio of Cu:R ; 70 µM of R). The drift time remained unchanged upon copper coordination, which indicates that both R2 dimer with and without copper coordination has relatively similar collision cross section.

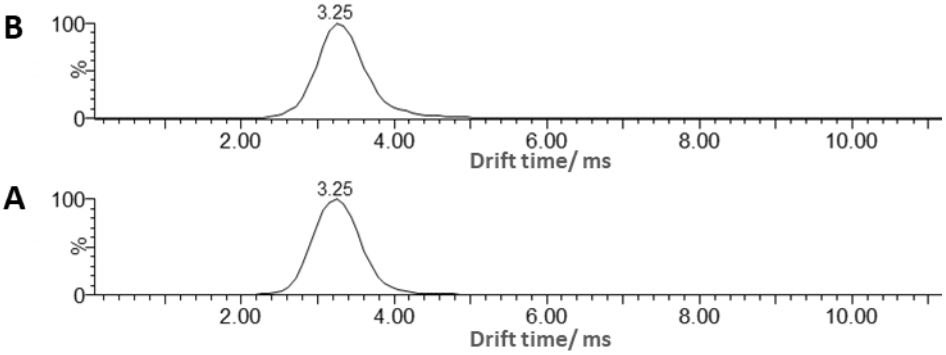

Figure S24. Drift time distribution as determined by ESI-IMS-MS for m/z corresponded to (A) $[2R2+6H]^{6+}$ and (B) $[2R2+Cu+3H]^{6+}$ (2:1 molar ratio of Cu:R; 70 µM of R). The drift time remained unchanged upon copper coordination, which indicates that both R2 dimer with and without copper coordination has relatively similar collision cross section.

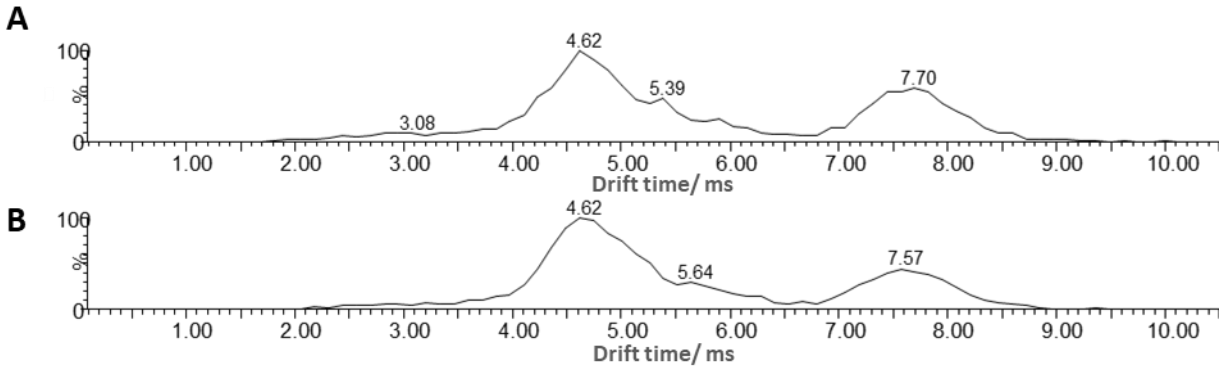

Figure S25. Drift time distribution as determined by ESI-IMS-MS for m/z corresponded to (A) $[2R3+4H]^{4+}$ and (B) $[2R3+Cu+2H]^{4+}$ (2:1 molar ratio of Cu:R; 70 µM of R). The drift time didn't change significantly upon copper coordination, which indicates that both R3 dimer with and without copper coordination has relatively similar collision cross section.

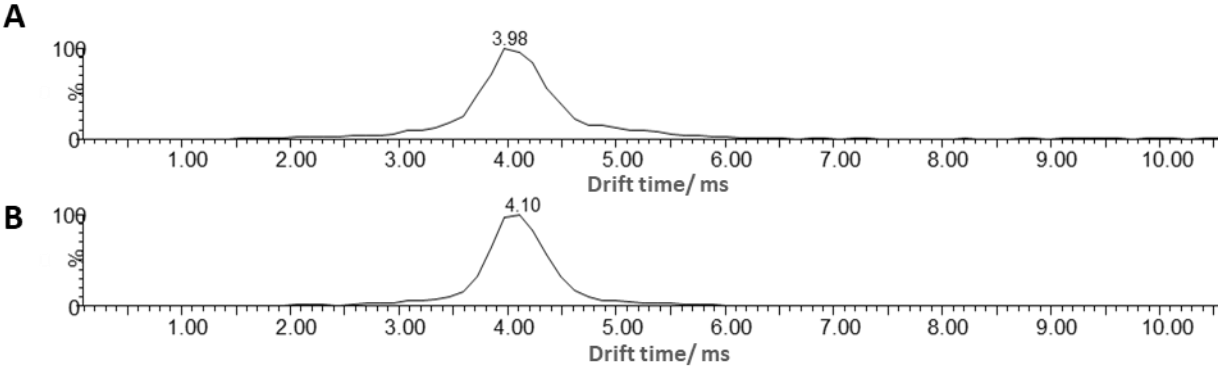

Figure S26. Drift time distribution as determined by ESI-IMS-MS for m/z corresponded to (A) $[2R3+5H]^{5+}$ and (B) $[2R3+Cu+3H]^{5+}$ (2:1 molar ratio of Cu:R; 70 µM of R). The drift time didn't change significantly upon copper coordination, which indicates that both R3 dimer with and without copper coordination has relatively similar collision cross section.

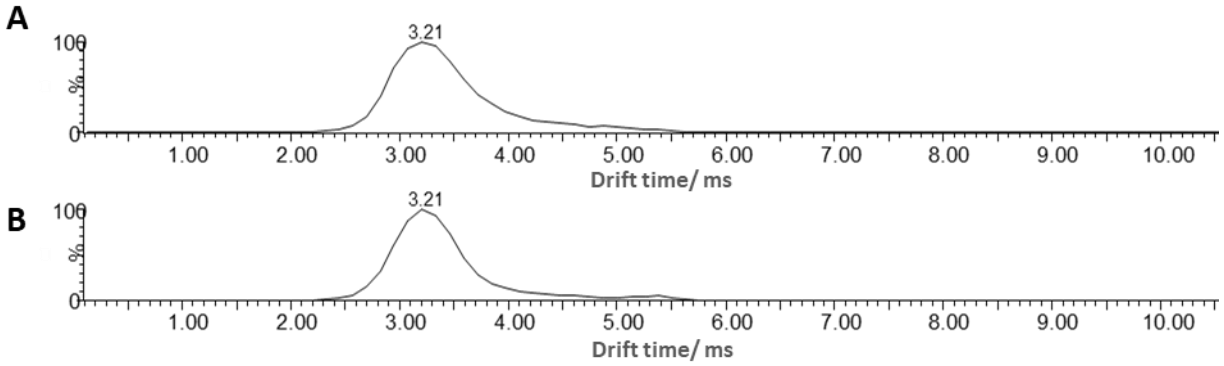

Figure S27. Drift time distribution as determined by ESI-IMS-MS for m/z corresponded to (A) $[2R3+6H]^{6+}$ and (B) $[2R3+Cu+4H]^{6+}$ (2:1 molar ratio of Cu:R; 70 µM of R). The drift time didn't change significantly upon copper coordination, which indicates that both R3 dimer with and without copper coordination has relatively similar collision cross section.

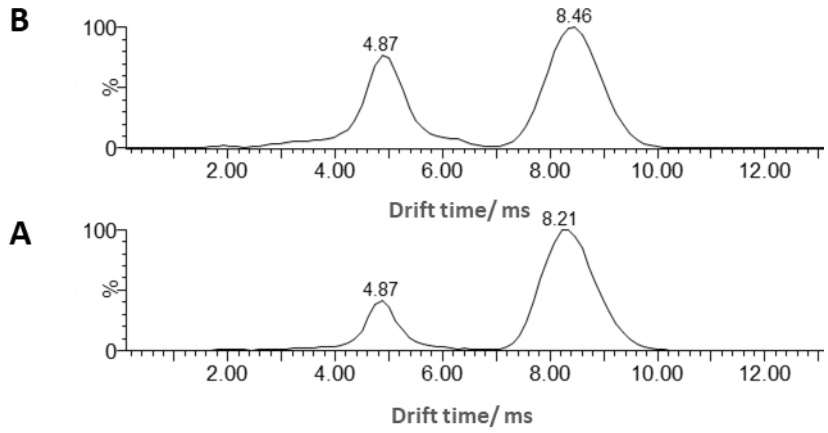

Figure S28. Drift time distribution as determined by ESI-IMS-MS for m/z corresponded to (A) $[R4+2H]^{2+}$ and (B) $[R4+Cu]^{2+}$ (2:1 molar ratio of Cu:R; 70 µM of R). The drift time did not change significantly upon copper coordination, which indicates that both R4 dimer with and without copper coordination has relatively similar collision cross section.

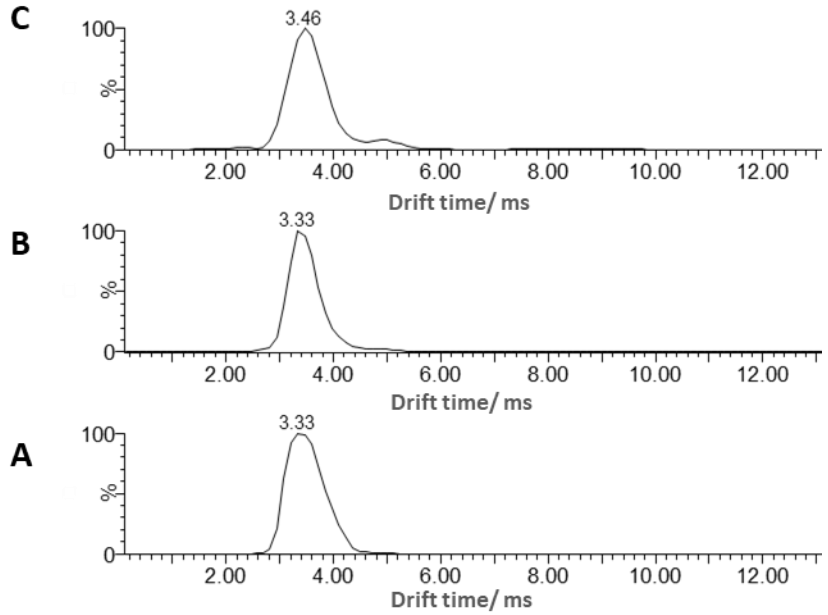

Figure S29. Drift time distribution as determined by ESI-IMS-MS for m/z corresponded to (A) $[R4+3H]^{3+}$, (B) $[R4+Cu+H]^{3+}$ and (C) $[R4+2Cu]^{2+}$ (2:1 molar ratio of Cu:R; 70 µM of R). The drift time did not change significantly upon copper coordination, which indicates that both R3 dimer with and without copper coordination has relatively similar collision cross section.

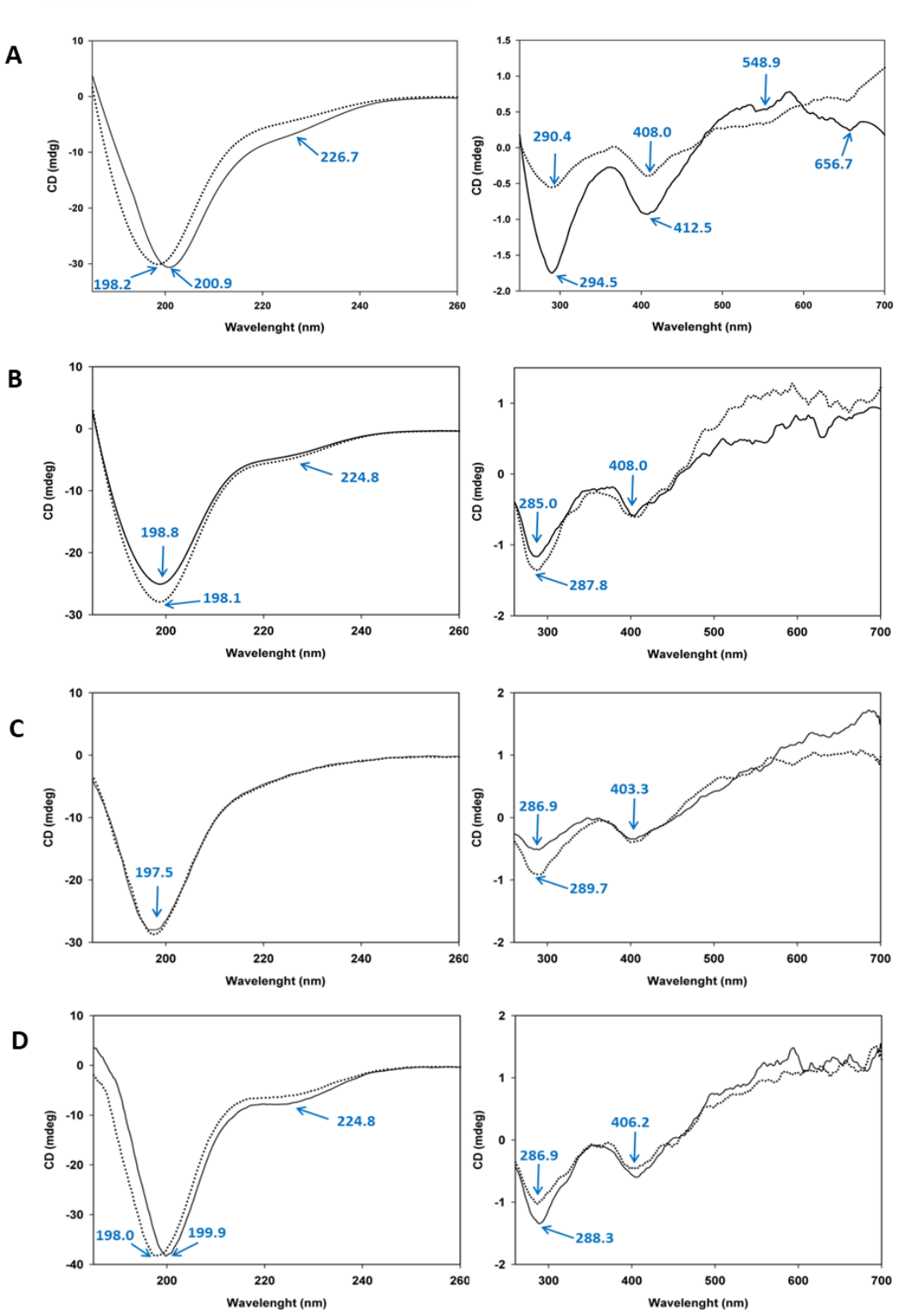

Figure S30. CD spectra (far UV left and UV-vis right) of 0.14 mM microtubule binding repeat R1 (A), R2 (B), R3 (C), and R4 (D) immediately after mixing with 0.28 mM Cu^{2+} solution at 25°C (pH 7.4) (solid line) and after 24 hours incubation at 25°C (dotted line). Each spectrum is the average of 3 scans.

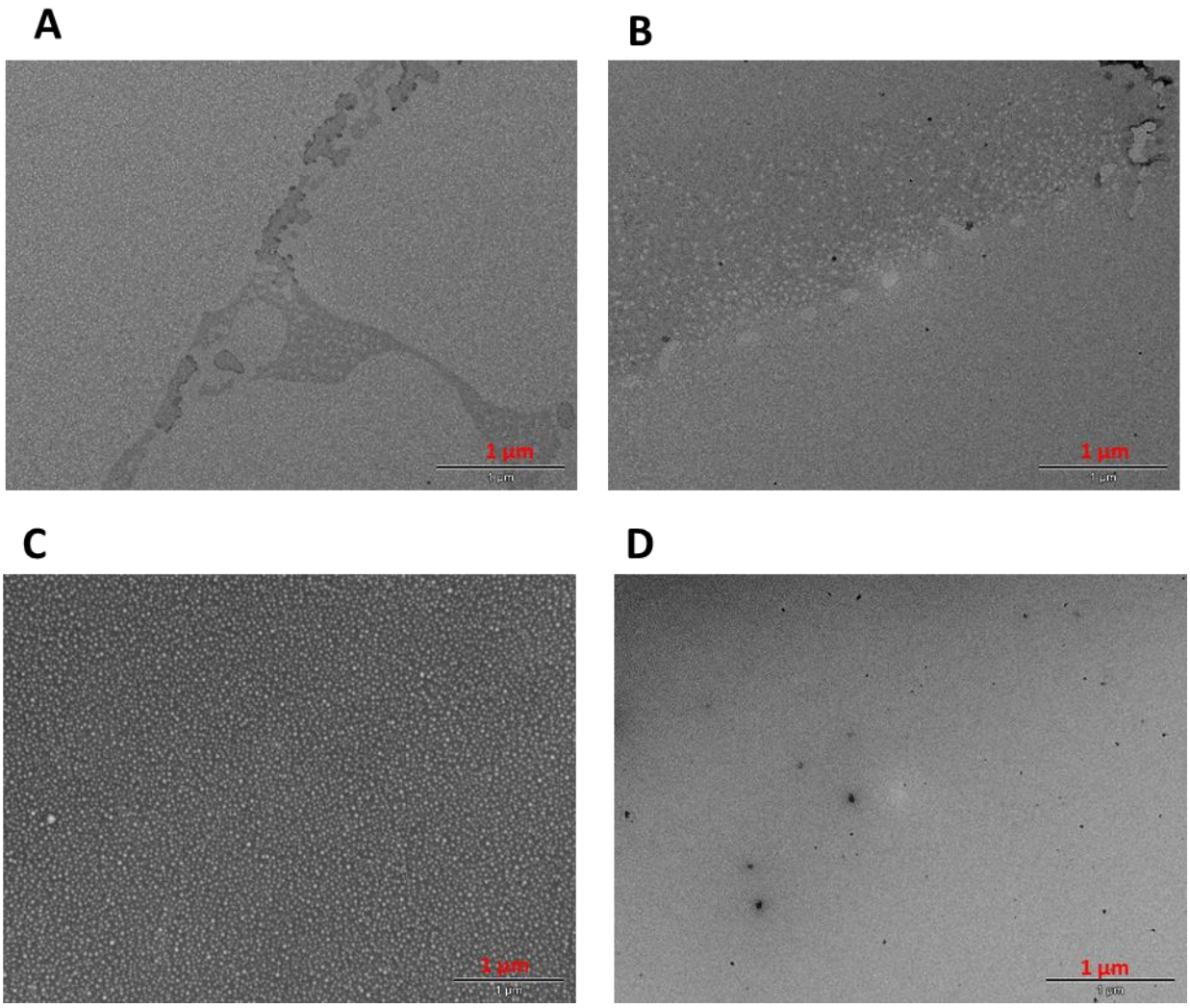

Figure S31. TEM images of R1 (A), R2(B), R3 (C), and R4 (D) after incubating at 25°C (pH 7.4) for 3 days. The images show that peptides slightly aggregate.

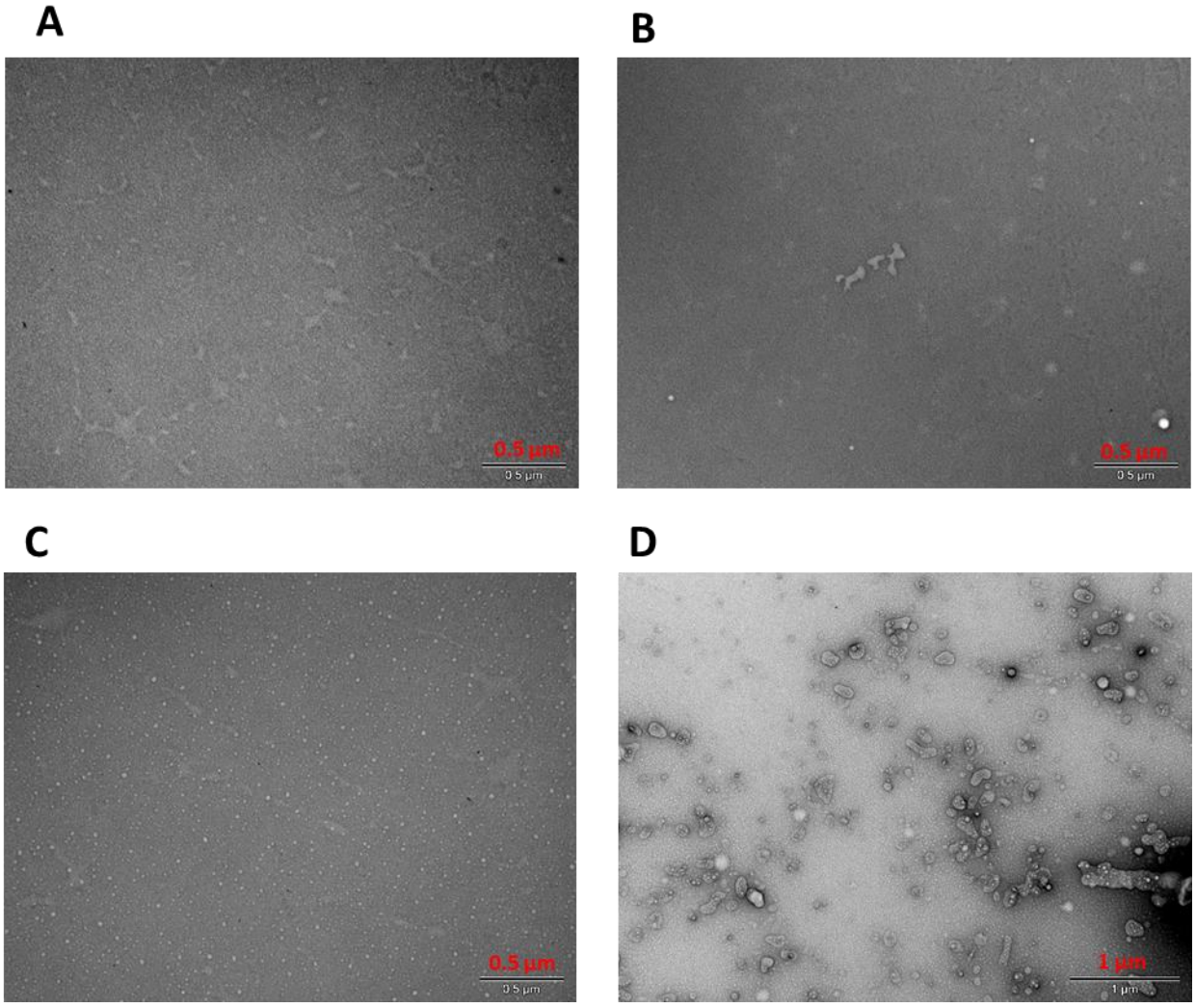

Figure S32. TEM images of R1 (A), R2(B), R3 (C), and R4 (D) after incubating at 25°C (pH 7.4) for 4 days. The images show that peptides slightly aggregate.

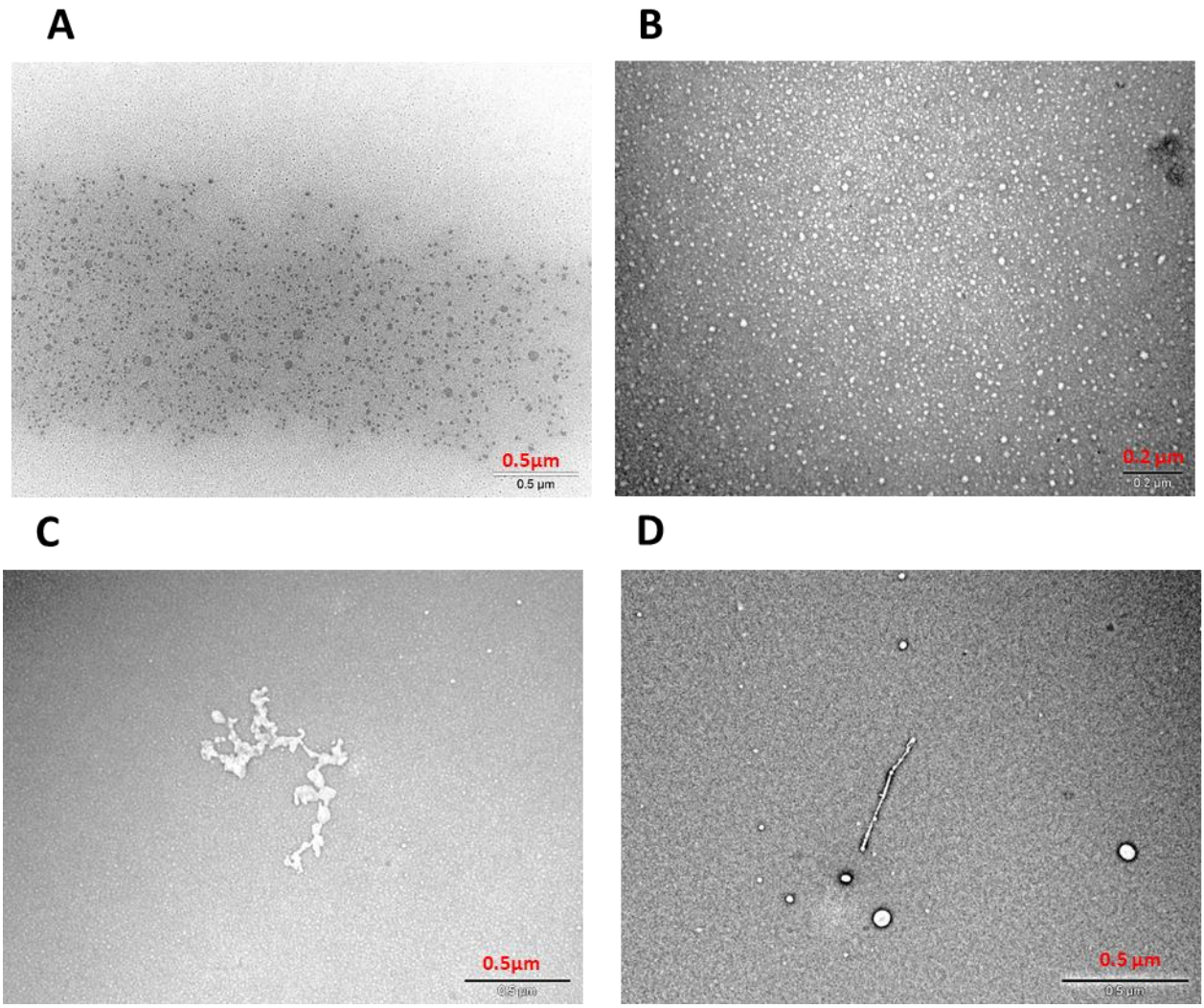

Figure S33. TEM experiment for the evaluation of the influence of Cu^{2+} on the aggregation of microtubule binding repeat R1 and R2. TEM images of R1 (A and B) and R2 (C and D) after incubating in Cu^{2+} solution at 25°C (pH 7.4) for 3 days. The images show the formation of oligomers and amorphous aggregates upon Cu^{2+} interaction.

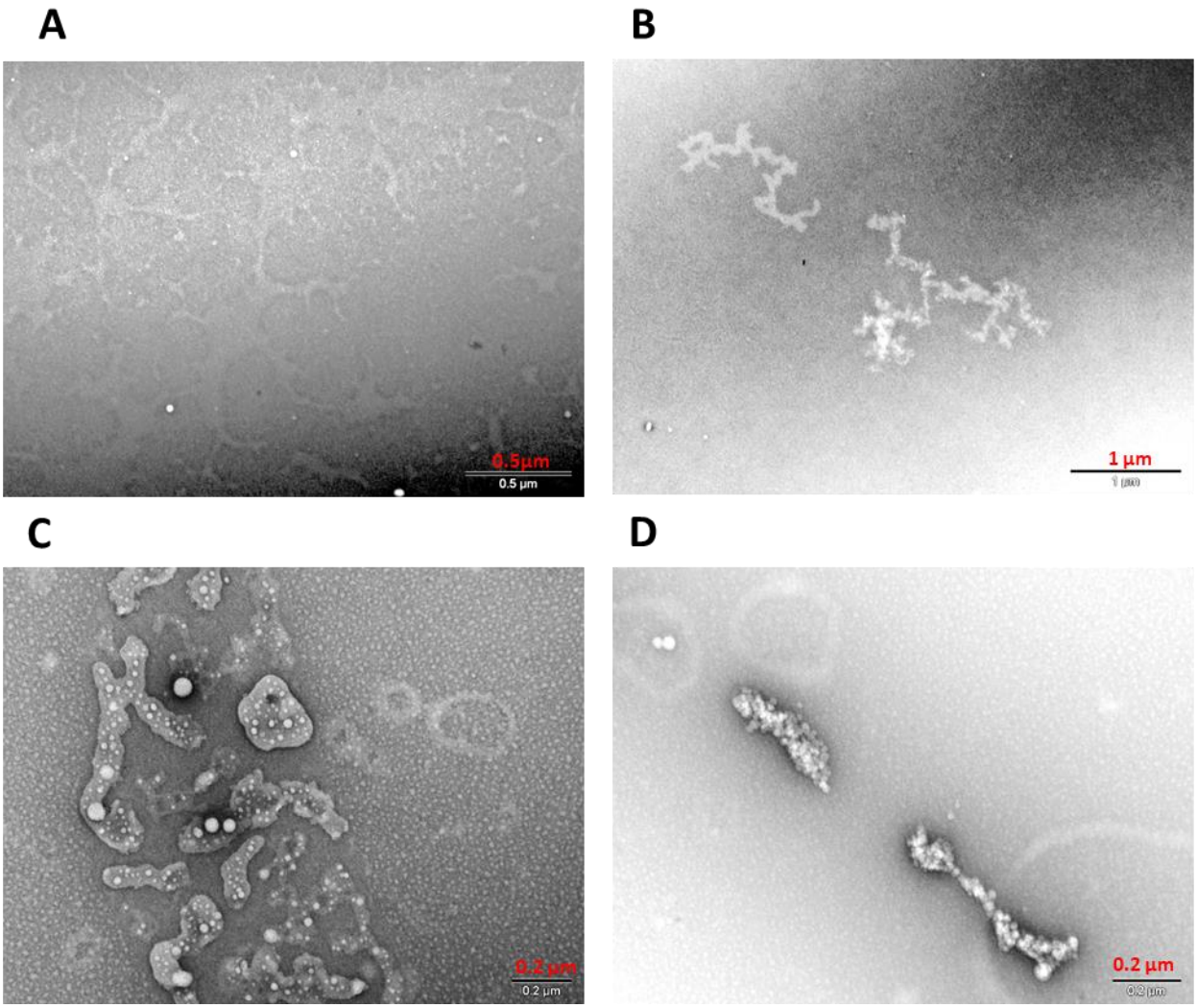

Figure S34. TEM experiment for the evaluation of the influence of Cu^{2+}on the aggregation of microtubule binding repeat R3 and R4. TEM images of R3 (A and B) and R4 (C and D) after incubating in Cu^{2+} solution at 25°C (pH 7.4) for 3 days. The images show the formation of amorphous aggregates upon copper interaction.

.

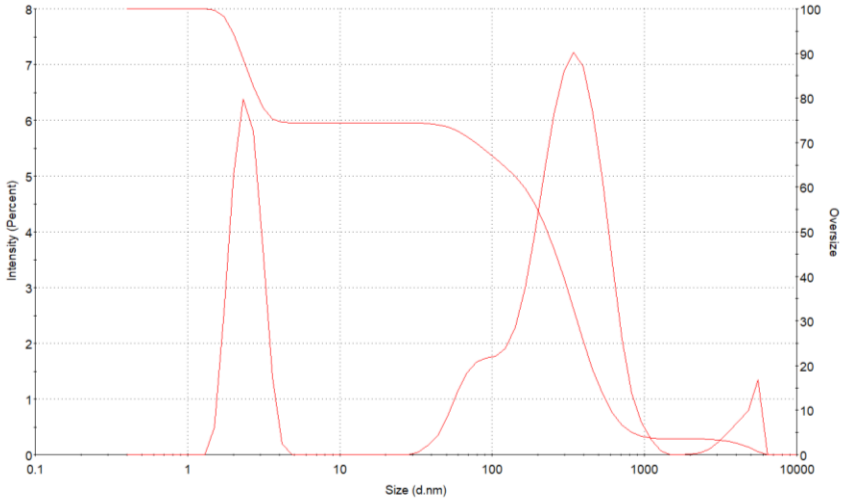

Figure S35. Size distribution plot obtaining from DLS experiment for R2 solution after incubating in Cu^{2+} solution (2:1 molar ratio of Cu:R) at 25°C (pH 7.4) for 4 days. DLS results show three different species with the average size of 2.47±0.05, 342±32 and 4518±233. (see table S2 for data)

Table S2. DLS results for R2 solution after incubating in Cu^{2+} solution (2:1 molar ratio of Cu:R) at 25°C (pH 7.4) for 4 days. DLS results show three different species.

R2-Cu	Size (d.nm)	Signal Intensity%	DLS	Estimated MW (KDa)
Peak 1	342±32	67±3	182±48	$5.7 \pm 1.2 \times 10^5$
Peak 2	2.5±0.1	26±2	0.53±0.07	5.5±2
Peak 3	4518±233	5±1	874±110	$2.4 \pm 0.3 \times 10^8$

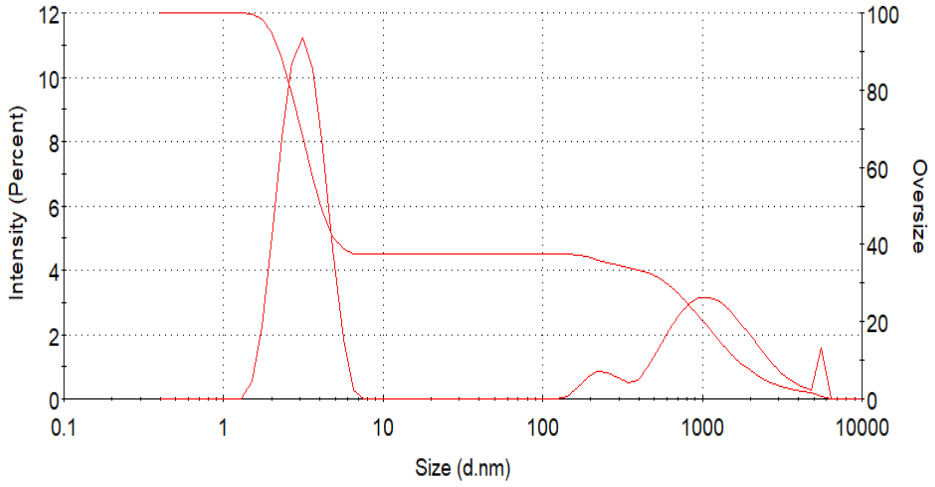

Figure S36. Size distribution plot obtaining from DLS experiment for R3 solution after incubating in Cu^{2+} solution (2:1 molar ratio of Cu:R) at 25°C (pH 7.4) for 4 days. DLS results show three different species with the average size of 3.22±0.08, 220±55 and 1003±662. (see table S3 for data)

Table S3. DLS results for R3 solution after incubating in Cu^{2+} solution (2:1 molar ratio of Cu:R) at 25°C (pH 7.4) for 4 days. DLS results show three different species.

R3-Cu	Size (d.nm)	Signal Intensity%	DLS	Estimated MW (KDa)
Peak 1	3.2±0.1	62±2	0.95±0.06	10.2 ±0.6
Peak 2	1003±662	36±2	610±501	2.2±0.8 $X10^7$
Peak 3	220±55	3.8±0.5	55.69	8.8±3.2 $x10^6$

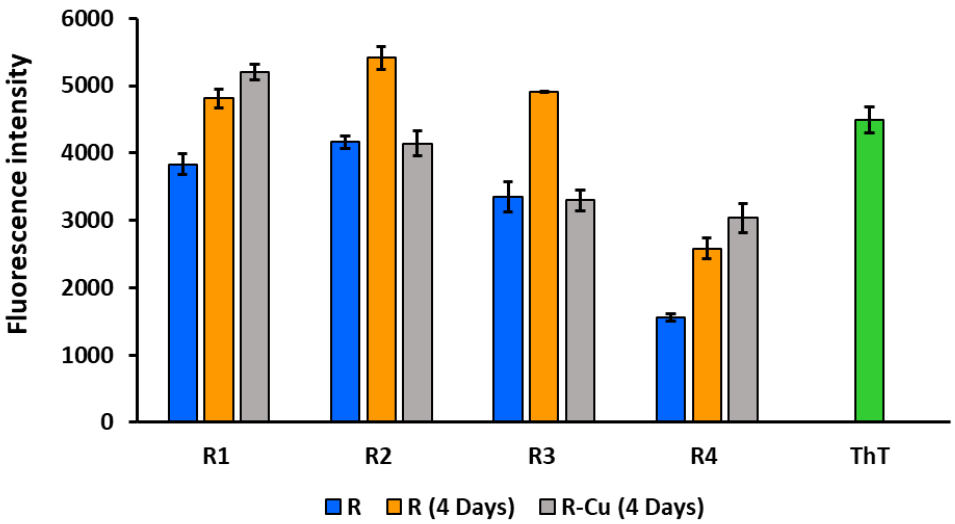

Figure S37. ThT fluorescence experiment for monitoring the β-sheet structure in MT binding repeats. Bar chart represents the ThT fluorescence intensity of the MT binding repeats R1-R4 (blue), after 4 days incubation with (gray) and without (orange) Cu^{2+} at room temperature. The green bar shows the ThT fluorescence of the control sample in the absence of peptide and Cu^{2+}. Error bars represent the standard deviation of three measurements.

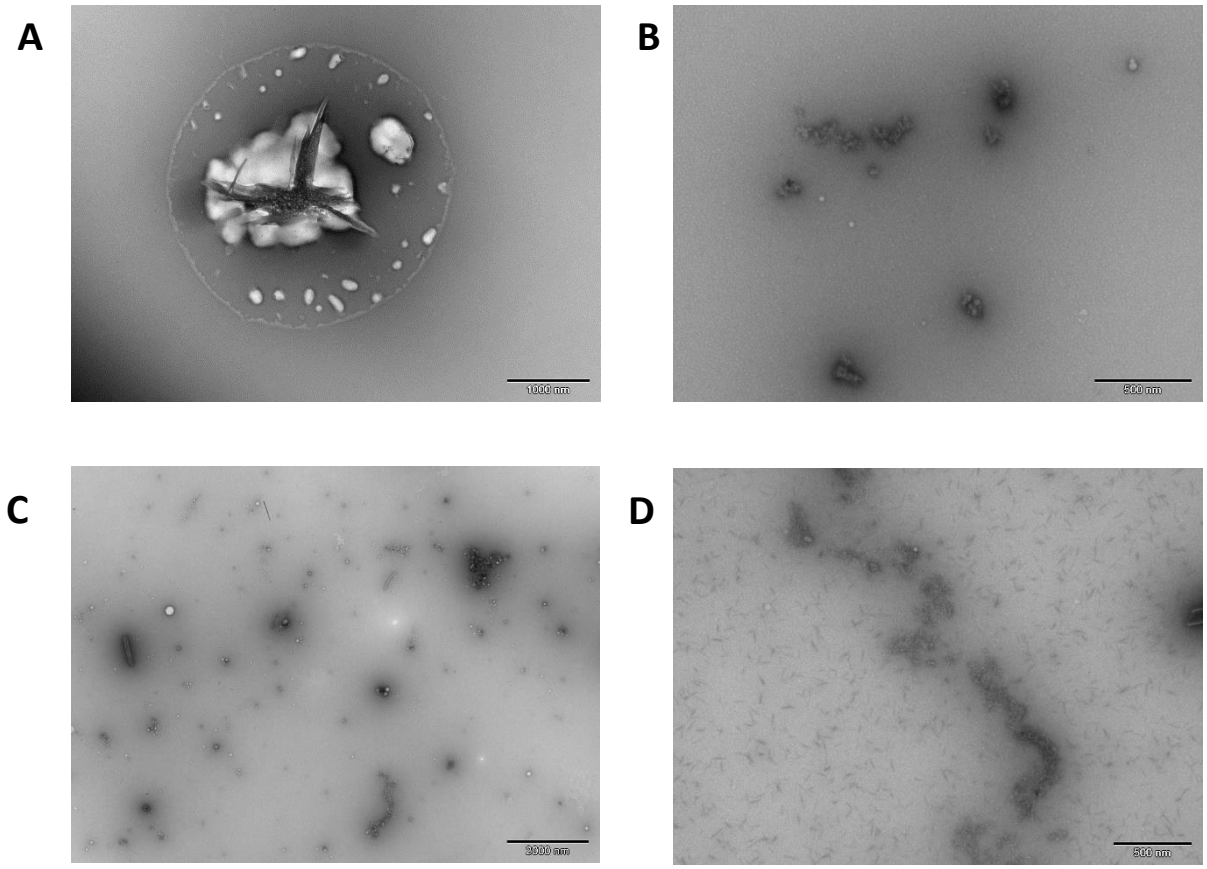

Figure S38. TEM experiment for the evaluating the impact of glutathione (GSH) on the interaction of microtubule binding repeats with Cu^{2+}. TEM images of R1 (A), R2 (B), R3 (C) and R4 (D) after incubation at 25°C (pH 7.4) for 4 days in Cu^{2+} and GSH (molar ratio of 1:2:1 for R:Cu:GSH) in limited access of oxygen. TEM images illustrate the different aggregation profiles of microtubule binding repeats in presence of Cu^{2+} and GSH, which suggested that GSH even in the limited access to oxygen do not inhibit the aggregation effect of Cu^{2+} on microtubule binding repeats.

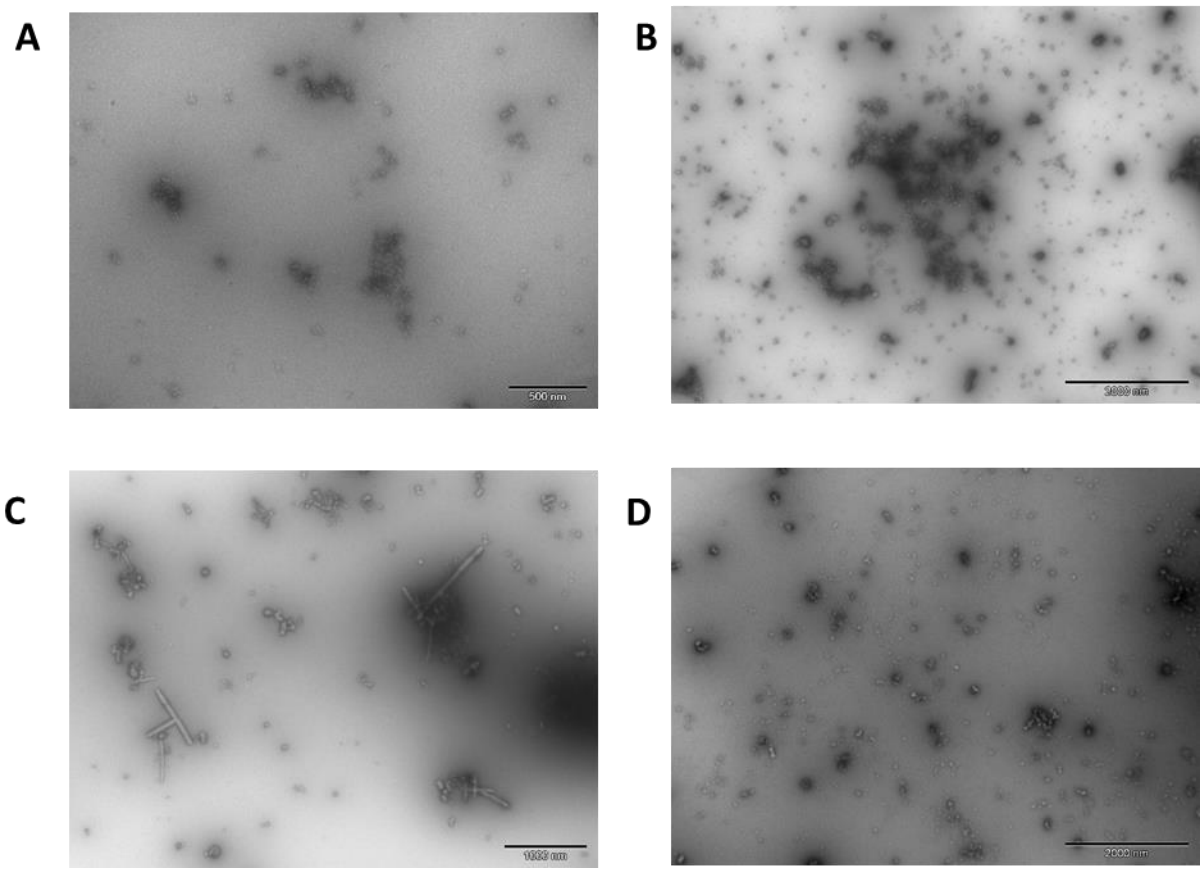

Figure S39. TEM experiment for the evaluating the impact of glutathione (GSH) on the interaction of microtubule binding repeats with Cu^{2+}. TEM images of R1 (A), R2 (B), R3 (C) and R4 (D) after incubation at 25°C (pH 7.4) for 4 days in Cu^{2+} and GSH (molar ratio of 1:0.5:10 for R:Cu:GSH) in ambient oxygen. TEM images illustrate the different aggregation profiles of microtubule binding repeats in presence of Cu^{2+} and GSH, which suggested that GSH not only do not inhibit the interaction of Cu^{2+} with microtubule binding repeats but also trigger the microtubule binding repeats aggregation in particular for R3.

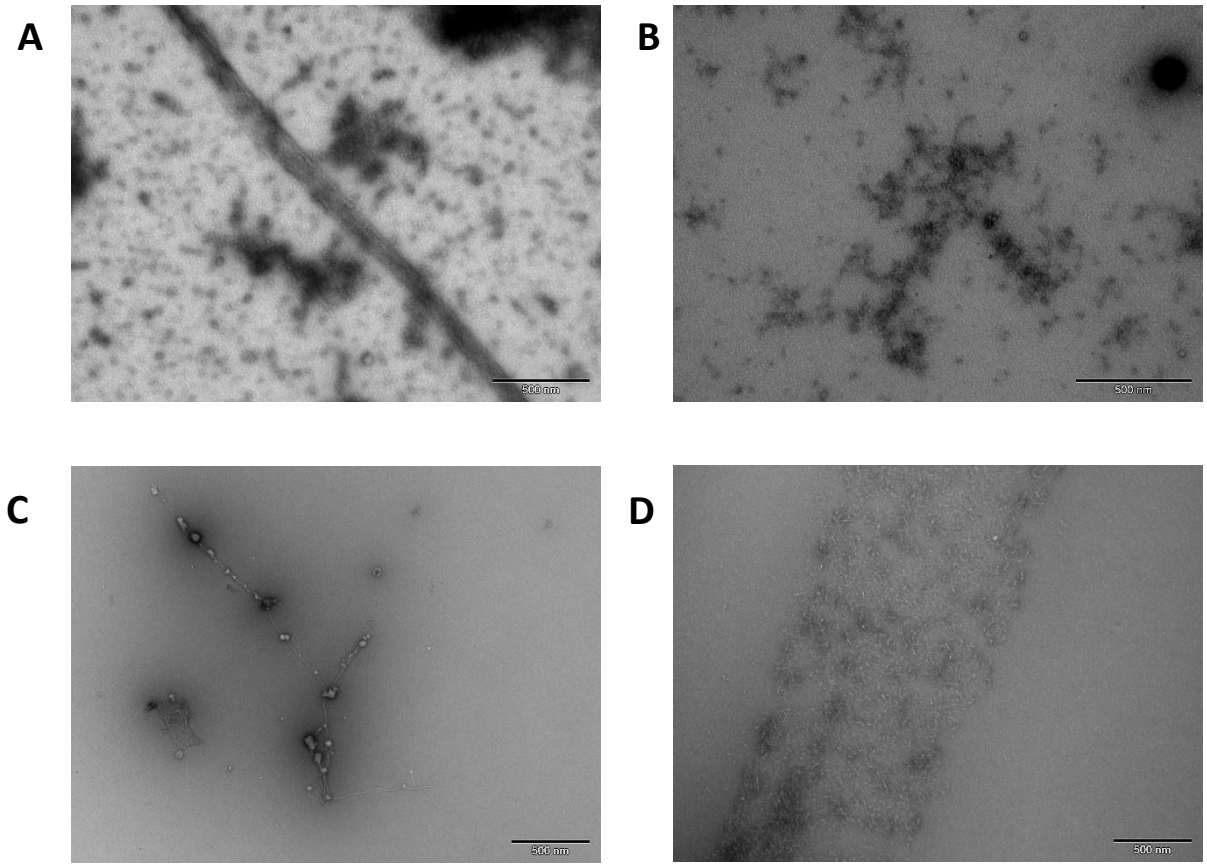

Figure S40. TEM experiment for the evaluating the impact of glutathione (GSH) and ascorbic acid on the interaction of microtubule binding repeat with Cu^{2+}. TEM images of R1 (A), R2 (B), R3 (C) and R4 (D) after incubation at 25°C (pH 7.4) for 4 days in Cu^{2+}, AA and GSH (molar ratio of 1:0.5:10:10 for R:Cu:GSH:AA) in ambient oxygen. TEM images illustrate the different aggregation profiles of microtubule binding repeats in presence of Cu^{2+} and GSH and in strong reducing environment, which suggested that even strong reducing environment do not prevent the interaction of Cu^{2+} with microtubule binding repeats.

References

1. Martić, S.; Beheshti, S.; Rains, M. K.; Kraatz, H.-B. Electrochemical investigations into Tau protein phosphorylations. Analyst. **2012**, 137 (9), 2042–2046.

2. Barghorn, S.; Biernat, J.; Mandelkow, E. Purification of recombinant tau protein and preparation of Alzheimer-paired helical filaments in vitro. Methods Mol. Biol. **2005**, 299, 35–51.

3. Zhu, S.; Shala, A.; Bezginov, A.; Sljoka, A.; Audette, G.; Wilson, D. J. Hyperphosphorylation of Intrinsically Disordered Tau Protein Induces an Amyloidogenic Shift in Its Conformational Ensemble. PLoS One. **2015**, 10 (3), 1–15.

4. Zhu, S.; Campbell, J. L.; Chernushevich, I.; Le Blanc, J. C. Y.; Wilson, D. J. Differential Mobility Spectrometry-Hydrogen Deuterium Exchange (DMS-HDX) as a Probe of Protein Conformation in Solution. J. Am. Soc. Mass Spectrom. **2016**, 27 (6), 991–999.

5. Simpson, A. J.; Brown, S. A. Purge NMR: effective and easy solvent suppression. J. Magn. Reson. **2005**, 175 (2), 340–346.

6. Takegoshi, K.; Ogura, K.; Hikichi, K. A perfect spin echo in a weakly homonuclear J-coupled two spin 12 system**.** J. Magn. Reson. **1989**, 84 (3), 611–615.

7. Wu, D. H.; Chen, A. D.; Johnson, C. S., An improved diffusion-ordered spectroscopy experiment incorporating bipolar-gradient pulses. J. of Magn. Reason. **1995**, 115 (2), 260–264.

8. Sakhaii, P.; Bermel, W. (2015) A different approach to multiplicity-edited heteronuclear single quantum correlation spectroscopy. J. of Magn. Reason. **2015**, 259, 82-86

9. Woods, G. C.; Simpson, M. J.; Koerner, P. J.; Napoli, A.; Simpson, A. HILIC-NMR: Toward the Identification of Individual Molecular Components in Dissolved Organic Matter. J. Environ. Sci. Technol. **2011**, 45 (9), 3880–3886.

10. Lebel, C. P.; Ischiropoulos, H.; Bondys, S. C. Evaluation of the probe 2',7'-dichlorofluorescin as an indicator of reactive oxygen species formation and oxidative stress. Chem. Res. Toxicol. **1992**, 5 (2), 227–231.

11. Cohn, C. a; Simon, S. R.; Schoonen, M. A. Comparison of fluorescence-based techniques for the quantification of particle-induced hydroxyl radicals. Part. Fibre Toxicol. **2008**, DOI:10.1186/1743-8977-5-2.

12. Ahmadi, S.; Ebralidze, I. I.; She, Z.; Kraatz, H. B. Electrochemical studies of tau protein-iron interactions—Potential implications for Alzheimer's Disease. Electrochim. Acta. **2017**, 236, 384–393.

13. Martic, S.; Rains, M. K.; Kraatz, H. B. Probing copper/tau protein interactions electrochemically. Anal. Biochem. **2013**, 442 (2), 130–137.

14. Peisach, J.; Blumberg, W. E. Structural implications derived from the analysis of electron paramagnetic resonance spectra of natural and artificial copper proteins**.** Arch. Biochem. Biophys. **1974**, 165 (2), 691–708.

15. Shin, B., and Saxena, S. Insight into potential Cu(II)-binding motifs in the Four pseudorepeats of Tau protein. J. Phys. Chem. B. **2011**, 115 (50), 15067–15078.